

70-16,840

DUNAWAY, Jr., George A., 1941-  
A COMPARATIVE STUDY OF SOME OF THE ASPECTS  
INVOLVED IN THE REGULATION OF GLYCOLYSIS IN  
HUMAN DIPLOID AND VIRAL TRANSFORMED CELLS.

The University of Oklahoma, Ph.D., 1970  
Biochemistry

University Microfilms, A XEROX Company, Ann Arbor, Michigan

THE UNIVERSITY OF OKLAHOMA  
GRADUATE COLLEGE

A COMPARATIVE STUDY OF SOME OF THE ASPECTS INVOLVED  
IN THE REGULATION OF GLYCOLYSIS IN HUMAN  
DIPLOID AND VIRAL TRANSFORMED CELLS

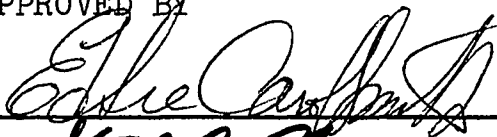
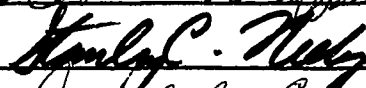

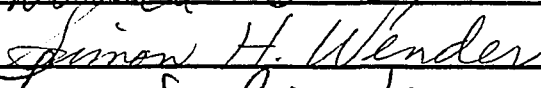
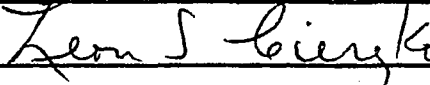
A DISSERTATION  
SUBMITTED TO THE GRADUATE FACULTY  
in partial fulfillment of the requirements for the  
degree of  
DOCTOR OF PHILOSOPHY

BY  
GEORGE A. DUNAWAY, JR.  
Norman, Oklahoma

1970

A COMPARATIVE STUDY OF SOME OF THE ASPECTS INVOLVED  
IN THE REGULATION OF GLYCOLYSIS IN HUMAN  
DIPLOID AND VIRAL TRANSFORMED CELLS

APPROVED BY

DISSERTATION COMMITTEE

## ACKNOWLEDGMENTS

The author wishes to express his sincere indebtedness to Dr. E. C. Smith for serving as major professor and chairman of the advisory committee and for his competent advice and insight which improved the quality of this research.

The author is grateful to the other members of his committee, Dr. Leon S. Ciereszko, Dr. Simon Wender, Dr. Stanley C. Neely, and Dr. Donald C. Cox for their counsel and assistance and for the use of their equipment and facilities.

The author appreciates the use of the tissue culture equipment which Dr. H. W. Larsh generously permitted.

The author wishes to express his thanks to the rest of the faculty and graduate students of the Chemistry and Microbiology Departments for their helpful advice and friendship.

The author would like to thank the Graduate School and National Science Foundation for endowing the author with a National Science Foundation Traineeship. The author

wishes to thank Mrs. Marjorie E. Bradley for her advice and concern with the administration of the traineeship.

The author cannot adequately express the debt that he owes to Dr. Paul F. Kruse and other members of the Samuel Roberts Noble Foundation, Inc. for their help in establishing and maintaining a tissue culture laboratory at the University of Oklahoma.

The author wishes to thank his parents, Mr. and Mrs. George A. Dunaway; grandmother, Mrs. Lola M. Clifton; brothers, Larry and Richard; and his mother and father-in-law, Mr. and Mrs. Denton Kilgo, for their moral and financial help. The author wishes to especially thank his wife, Susan, and son, John, for the love and understanding that eased the pressure of graduate school.

## TABLE OF CONTENTS

	Page
LIST OF TABLES . . . . .	vi
LIST OF ILLUSTRATIONS. . . . .	vii
Chapter	
I. INTRODUCTION AND LITERATURE SURVEY . . . . .	1
II. PURPOSE AND SCOPE. . . . .	15
III. EXPERIMENTAL MATERIALS AND METHODS . . . . .	16
IV. EXPERIMENTAL RESULTS . . . . .	31
V. DISCUSSION . . . . .	74
VI. SUMMARY. . . . .	97
BIBLIOGRAPHY . . . . .	100

## LIST OF TABLES

Table	Page
1. Glucose Consumption and Lactate Production in WI-38 and WI-38 VA13A . . . . .	31
2-A. Levels of Adenine Nucleotides in WI-38 VA13A . .	32
2-B. Levels of Adenine Nucleotides in WI-38 . . . . .	33
3-A. Enzyme Patterns in WI-38 . . . . .	35
3-B. Enzyme Patterns in WI-38 VA13A . . . . .	36
4. A List of Interaction Coefficients . . . . .	38
5. pH Optima. . . . .	39
6. Kinetic Constants Tabulated from Figures 1-25. .	68
7. Effect of Selected Compounds on the Activity of HK, PK, GAPDH, and GPDH . . . . .	71
8. Comparison of the HK Levels and Glucose Consumption for WI-38 and WI-38 VA13A. . . . .	76
9. Order of Increasing Glycolytic Enzyme Activity for WI-38, WI-38 VA13A, and Human Lung . . . . .	83

## LIST OF ILLUSTRATIONS

Figure	Page
1. Glucose Saturation of HK from WI-38 and Corresponding Lineweaver-Burk Plot (inset). .	40
2. Glucose Saturation of HK for WI-38 VA13A and Corresponding Lineweaver-Burk Plot (inset) . . . . .	41
3. ATP Saturation of HK from WI-38 and Corresponding Lineweaver-Burk Plot (inset). .	42
4. ATP Saturation of HK from WI-38 VA13A and Corresponding Lineweaver-Burk Plot (inset). .	43
5. G-6-P Saturation of GPDH from WI-38 . . . . .	44
6. Lineweaver-Burk Plot of G-6-P Saturation of GPDH from WI-38. . . . .	45
7. G-6-P Saturation of GPDH from WI-38 VA13A . . .	46
8. Lineweaver-Burk Plot of G-6-P Saturation of GPDH from WI-38 VA13A. . . . .	47
9. $\text{NADP}^+$ Saturation of GPDH from WI-38 . . . . .	48
10. $\text{NADP}^+$ Saturation of GPDH from WI-38 VA13A . . .	49
11. GAP Saturation of GAPDH from WI-38. . . . .	50
12. GAP Saturation of GAPDH from WI-38 VA13A. . . .	51
13. $\text{NAD}^+$ Saturation of GAPDH from WI-38 . . . . .	52
14. $\text{NAD}^+$ Saturation of GAPDH from WI-38 VA13A . . .	53
15. Effect of ATP on PEP Saturation of PK from WI-38 . . . . .	54



Figure		Page
16.	Effect of L-Alanine on PEP Saturation of PK from WI-38 . . . . .	55
17.	Effect of L-Alanine (top curve) and ATP (lower curve) on Lineweaver-Burk Plot for PEP Saturation of PK from WI-38 . . . .	56
18.	Effect of L-Alanine and ATP on PEP Sat- uration of PK from WI-38 VA13A. . . . .	57
19.	Effect of L-Alanine and ATP on Lineweaver- Burk Plot for PEP Saturation of PK from WI-38 VA13A . . . . .	58
20.	Effect of FDP on PEP Saturation of PK from WI-38 VA13A . . . . .	59
21.	Effect of ATP on ADP Saturation of PK from WI-38 . . . . .	60
22.	Effect of L-Alanine on ADP Saturation of PK from WI-38 . . . . .	61
23.	Effect of L-Alanine (top curve) and ATP (lower curve) on Lineweaver-Burk Plot for ADP Saturation of PK from WI-38 . . . .	62
24.	Effect of ATP on ADP Saturation of PK from WI-38 VA13A. . . . .	63
25.	Effect of L-Alanine on ADP Saturation of PK from WI-38 VA13A . . . . .	64
26.	Activation of PK from WI-38 and WI-38 VA13A by KCl. . . . .	65
27.	Desensitization of PK from WI-38 VA13A to FDP Activation by Storage at -20°C . . .	66

A COMPARATIVE STUDY OF SOME OF THE ASPECTS INVOLVED IN  
THE REGULATION OF GLYCOLYSIS IN HUMAN DIPLOID  
AND VIRAL TRANSFORMED CELLS

CHAPTER I

INTRODUCTION AND LITERATURE SURVEY

The transformation of cells by oncogenic viruses probably offers the best "in vitro" opportunity for determining the early events of neoplastic conversion. Cells may be transformed by ribonucleic acid (RNA) and deoxyribonucleic acid (DNA) containing viruses, and the character of the transformation is dependent upon the type of interaction that these viruses make with the cells which they transform. The RNA containing viruses that can effect viral transformation are the murine leukemic and avian leukosis groups, and the DNA containing viruses capable of inducing cell transformation are polyoma virus, the vacuolating simian virus (SV40) and certain adenoviruses. RNA viral transformation may be subdivided into two groups based on the formation of infectious virus. In the murine leukemic and certain avian leukosis groups, the virus continues to be produced by the tumor and released into the medium by

budding. In the Rous sarcoma viral transformed cell, very little, if any, infective virus is found. Transformation of cells by DNA oncogenic viruses results in no detectable viruses in cell extracts. The DNA and Rous sarcoma viral transformations differ in that for the DNA viral transformed cells viruses can only be induced in exceptional cases, and for Rous sarcoma viral transformed cells infectious virus can be readily obtained under the proper conditions. For example, when the Bryan high titer strain of Rous sarcoma virus is used to transform chicken cells, superinfection with a helper virus of the avian leukosis group leads to formation of infectious viruses. The helper virus promotes infection by synthesizing the protein coat that can not be produced by the Rous sarcoma virus. Interaction of the Schmidt-Rubin strain of Rous sarcoma virus with mammalian cells leads to transformed mammalian cells which do not release virus until the cells are cultured with chick embryo cells (24).

Since the transformed cells used in this research project were transformed by SV40, it is pertinent to consider the literature in some detail on viral transformation by SV40. Infection of new born hamsters with SV40 resulted in the formation of malignant tumors at the injection site (20, 23). The discovery of this oncogenic agent prompted a study on the behavior of human tissue exposed to infection with SV40. Biopsies of buccal mucosa and skin

from adult male and female humans were cultured and infected with SV40 (34). Initially no morphologic differences were observed in either the infected or noninfected cells, and both cell types readily formed monolayers. Between eight and fourteen weeks the first visible indication of a change in the infected and virus yielding cultures was the appearance of areas of tightly packed and linearly arranged cells. Numerous cells exhibited perinuclear granulation and were in mitosis. Further passages of these cells resulted in increasing numbers of colonies of the transformed cells with the non-transformed cells finally disappearing. The transformed cells exhibited an epithelial-like morphology in contrast to a fibroblast-like morphology for non-transformed cells. In addition, transformed cells were irregular, polymorphic, and had large nucleoli. If both cell types were provided equal surface areas on which to form confluent sheets, approximately two-fold to three-fold more cells were found in the cultures of the transformed cells which indicates either smaller cells, tighter packing, or multilayers of cells. Also, considerably more mitotic activity occurred in the transformed cells, and the transformed cells were found to have a greater growth rate than non-transformed cells. The viral transformed cells were also found to have an abnormal karyotype, but the non-transformed cells were karyotypically normal. Continued passage of the transformed cells has indicated that the transformation did

not produce reversible phenotypes which was suspected since chromosomal aberrations accompany the transformation (34).

Since earlier work on SV40 transformation was done with an organ culture that originally contained epithelial cells, transformations of a pure strain of human fibroblasts were necessary to prove whether the fibroblasts were a result of selection of the original organ fibroblasts or of viral transformation. The following work was initiated to clarify this problem (4). It was found in contrast to organ cultures that in cell cultures the morphological transformation of fibroblasts to epithelioid cells was gradual. This transformation was characterized by formation of an undifferentiated rapidly dividing, aneuploid population that was well adapted to "in vitro" cultivation. Examination of the nucleoli indicated an excess of DNA around it and it was speculated (47) that disturbance of the nucleolus may play an important role in the SV40 transformation. Some of the transformed cell lines were found to have ceased viral shedding, but they were exceptions. The SV40 antigen present in a small fraction of the transformed cells was always shown by immunofluorescence to be present in the nucleolus. The conclusion from this work was that the fibroblasts were formed as a result of viral transformation. Later work on SV40 transformation of human diploid cells revealed the characteristic features of the phases of crises and recovery of SV40 induced transformation (22). These authors found,

as was previously reported, that SV40 transformed cells underwent morphological change, accelerated growth rate, and an extended survival beyond the life span characteristic of human diploid cells in culture. However, extended observation indicated that four to eight months after transformation, the ability to proliferate declined and the transformed cells displayed abnormal mitosis. The period of time that the cells indicated minimal survival was defined as "crisis." Following the "crisis" a new type of cell emerged which could be easily subcultured. If the transformed cells were assayed for infectious SV40 periodically before and during crisis, some virus was always detected, but after recovery no virus could be detected. Also, a new cellular protein was revealed by complement-fixation. This SV40 induced complement-fixing antigen distinct from the viral antigen was found in high titer after recovery as well as before crisis. Presence of this antigen in subsequent progeny indicated that it was an inheritable trait and may indicate either integration of viral genetic material or derepression of genetic material in the host cell. A more complete discussion of this antigen will be presented after the following discussion on the evidence for the presence of the viral genome persisting in the viral transformed cell.

Hybridization experiments with DNA from SV40 transformed hamster cells (SV3T3) and labeled virus specific RNA were performed on membrane filters by the Gillespie-

Spiegelman procedure (63). It was hoped that enough of the viral genome would be present in the transformed cells' DNA to hybridize with virus specific RNA. The virus specific RNA was made using viral DNA as a template with *Escherichia coli* RNA polymerase. The results of the experiments indicated about five to twenty SV40 DNA molecules per cell. The second project of this study involved the fusion of SV3T3 cells with BSC-1 cells which was accomplished using ultra-violet irradiated Sendai virus as the fusing agent. Although the SV3T3 cells do not produce virus about ten percent of the fused cells produced infectious SV40. These results indicated that integration of the viral genome was reversible and that complete viral genomes could be integrated into the SV3T3 cells (63). A similar study by Dulbecco's group compared the viral RNA synthesized in BSC-1 cells lytically infected with SV40 with RNA synthesized in SV3T3 cells (57). In the transformed cells it was found that one-third of the viral DNA was expressed as RNA, and the transcribed genes overlapped mostly with the SV40 genes active during early lytic infection. These findings were indicative that, at the most, one-third of the total viral genome was essential for transformation which corresponded roughly to two or three genes. These findings also strongly suggested that the late functions in the SV40 lytic cycle were irrelevant for transformation (57).

Recently, it has been reported that human diploid cells could be transformed by DNA extracted from SV40. The absorption of the DNA was mediated by incubation of the human cells and SV40 DNA with diethylaminoethyl dextran. The transformed cells produced SV40 T-antigen, were epitheloid, showed loss of contact inhibition of cell division and readily formed multiple cell layers. Persistent nuclear abnormalities and giant cells were also found (1).

As was discussed earlier specific antigens are demonstrable in virus induced tumors and cells transformed "in vitro" by viruses. These antigens may be divided into two categories, viral and cellular antigens. Viral antigens consist of structural proteins which are part of the intact virus. Cellular antigens are induced in the cell as a result of transformation but are not incorporated into the mature virus. In cells transformed by DNA viruses only cellular antigens are observed; however, in cells transformed by RNA viruses both cellular and viral antigens are found (24). The cellular antigens belong to one of two general sub-categories based on the immunological technique used for detection of the antigen. They are the transplantation type and serological type antigens. The transplanatation type antigen refers to the antigenically different cell surface that elicits an immunological reaction by the host animal to its own virus induced tumor. The serological type antigens are determined by serological techniques and are



postulated to be the early virus-induced enzymes involved in DNA synthesis since these antigens appear at the same time as the increase in certain enzymes involved in virus-induced cellular DNA synthesis. The appearance of specific antigens in transformed cells is now accepted as a general phenomenon, and although not directly shown, it is likely that their biosynthesis is coded by a persisting viral genome or at least a part of the viral genome. An interesting feature of these antigens is that their specificity is dependent on the original inducing virus and that they are present in all viral induced tumors regardless of the species of the host (24).

Next it is of interest to consider the characteristics of the human diploid cell strains. In 1961 Hayflick and Moorhead coauthored a paper that described certain criteria for the serial cultivation of human diploid cell strains (26). Up to that time only limited success had been obtained in cultivating human diploid cells "in vitro" over long periods of time. Since diploid cells parallel more closely the "in vivo" karyotype, their development would offer cell strains that should parallel more closely the "in vivo" biology of cells. Their paper also stresses the need for clarification of terminology used in tissue culture. The term cell strain defines a population of cells derived from animal tissue which has been cultivated more than once "in vitro," has a defined life span, and maintains one

diploid karyotype characteristic of the source tissue throughout its "in vitro" life span. Conversely, a cell line is a population of cells derived from animal tissue and grown "in vitro" by serial subcultivations for indefinite periods of time with a departure from the chromosome number characterizing its source. The term primary cells should indicate those cells obtained from the original source that have been cultivated "in vitro" for the first time. Thus the properties that primary cells assume after subsequent passages determine whether the cells are defined as a cell strain or as a cell line. These authors report successful cultivation of 25 human diploid cell strains from lung, muscle, skin, kidney, thymus, and heart. All the cells maintained a diploid karyotype and fibroblastic morphology throughout a finite "in vitro" life span. In general, the nucleus contains one to four nucleoli which vary from oval to branched bodies, and multinucleated cells are rarely found. The cells are transparent with fine cytoplasmic granularity, and the cell membrane is filamentous. "In vitro" these fibroblasts are extremely elongated, averaging about 185 microns by 15 microns. The confluent sheet is composed of swirls of cells with each cell aligned in a common direction. Gradually with continued transfers the cells change from an active mitotic state to a less active mitotic state and begin to accumulate debris. Also, the cells display less differences in the length of the axes and

lose contact inhibition. Various attempts to recover the cells e.g. medium changes or subcultivations always fail. From these observations it is evident that the life history of a cell strain may be characterized by three distinct phases. Phase I, or the early growth phase, denotes that period of time when the primary cells are introduced to tissue culture until the first confluent sheet is formed. Phase II is characterized by rapid cell multiplication and acid production. Phase III or the terminal phase is characterized by the appearance of debris and reduced mitotic activity which is manifested in tissue culture by longer periods of time required for confluency. A large majority of Phase III cells remain diploid, but bizarre nuclear forms and sizes are frequently observed (26).

The previous discussion of human diploid cells and their SV40 viral transformation has been of a general nature, and applies only generally to the cells used for this research project. Thus, a discussion concerning the cells used in this research is pertinent. The cells which were chosen for this research project were the human diploid cell strain WI-38 and its SV40 transformed counterpart WI-38 VA13A. WI-38 was originally cultured by Hayflick from human male embryonic lung tissue. WI-38 has the general characteristics of human diploid cells. They maintain diploidity throughout their life span and exhibit fibroblast-like morphology. Also, they exhibit the Phase III

phenomenon, but their "in vitro" life span is of sufficient length to permit them to be a practical research tool. In fact WI-38 is sold as a commercial cell strain by many tissue culture companies.

Infection of WI-38 with SV40 transforms it to a cell type that originally produces infectious SV40; however, in approximately five months the crisis stage results in a drastic drop in cell number. The cell line, WI-38 VA13A, was originated from the cells which survived the crisis period. These transformed cells are heteroploid and exhibit an epithelial-like morphology. Also the transformed cells have the antigenic properties characteristic of cells transformed by DNA viruses. It was noted independently by two research groups that for Phase III cells a shorter time elapsed between infection and transformation than for Phase II cells (31, 54). The reason for this enhanced transformation has not been established, but it could be due to an increased efficiency of adsorption and penetration by the virus.

Previous work has shown that WI-38 glycolysis proceeded at a uniform rate which was directly dependent on cell division and respiration rate (16, 37). Even though WI-38 cells exhibit lower mitotic activity while in Phase III, their total respiration, glucose respiration, and glycolytic capacity was not significantly altered from that observed for Phase II cells. Also, the predominate

fate of glucose remained lactic acid production (17). In perfusion systems there were trends which indicate that WI-38 VA13A. Since the data were scattered, it was not possible to state whether the two cell types were statistically different (36).

Glucose metabolism has been studied for other virus transformed cells. Glucose metabolism has been studied in Rous sarcoma tumors grown in chickens (4). The following conclusions could be made concerning the overall metabolism of the Rous sarcoma tumor: (1) Glucose was readily utilized and its rate of utilization was increased with increasing concentrations of glucose, and (2) the hexose monophosphate shunt was operative, but the maximum contribution of this route did not exceed four percent of the glucose used. Between 15 to 20 percent of the consumed labeled pyruvate could be accounted for as carbon dioxide, and no significant incorporation of labeled carbon from pyruvate was observed in the tissue glycogen (4). A comparative study of the glucose metabolism in BHK21 cells and Rous sarcoma virus transformed BHK21 cells indicated that the transformed cells have a two fold greater glucose consumption than the non-transformed cells (9). In more recent work it was found that cells transformed by Rous sarcoma viruses had the same over-all glycolytic capacity as uninfected chick embryo cells. However, the viral transformation conferred on the cells a greater potential for growth and glycolysis under

conditions that limited the growth of untransformed BHK21 cells e.g. serum depletion, growth in suspension culture and thymidine blockage (52).

Several enzymatic studies have been made which compared the enzymatic activity of transformed cells with non-transformed cells. Weber and coworkers compared several enzyme activities of 10 to 16 day chorio-allantoic membranes with Rous sarcoma transformed membrane (58). They found no significant differences in the specific activities (measured in micromoles of substrate utilized per hour per average cell  $\times 10^8$ ) for fructose diphosphatase, glucose-6-phosphate dehydrogenase, and 6-phosphogluconate dehydrogenase. However, for the viral induced tumor they found approximately four fold increases in phosphoglucomutase and lactate dehydrogenase specific activities as well as a two fold increase in the specific activity of phosphoglucoisomerase. Using BHK21 cells and polyoma virus transformed BHK21 cells, there was consistently higher aerobic and anaerobic glycolysis in the transformed cells. Enzymatic comparisons of these two cell types indicated higher hexokinase,  $\text{NADP}^+$  specific-isocitrate dehydrogenase, and malic dehydrogenase activities in the transformed cells, but lower G6PDH activity in the transformed cell (46). Cristofalo and coworkers have demonstrated that alkaline phosphatase activity is about three fold higher in WI-38 VA13A when compared to WI-38, while the activities of acid phosphatase and lactate

dehydrogenase are not statistically different in both cell types (15, 18). More recently he has reported that hexokinase is the rate limiting enzyme for glucose utilization in both cell types, and of the glycolytic enzymes only glucose phosphate isomerase was significantly different (approximately two fold higher in WI-38 VA13A). Also, 6-phosphogluconate dehydrogenase and transaldolase activities were about twice as high in WI-38 as in WI-38 VA13A (14).

## CHAPTER II

### PURPOSE AND SCOPE

From the reviewed literature it is evident that the biology of virus induced cells as well as their gross glycolytic and respiration rate has been partly studied. However, relatively few studies have been made correlating any observed differences in glycolysis with intercellular differences between the transformed and untransformed cells.

The goal of this research is to make a comparative study of the glycolytic capacities of human diploid and SV40 viral transformed cells and to explain any variation in glycolysis on the basis of enzyme profiles and/or response of certain enzymes to substrate and some regulatory effectors which are thought to control cellular glycolysis. It is hoped that the results of this research may be useful in understanding intercellular alterations that accompany neoplastic transformation.



## CHAPTER III

### EXPERIMENTAL MATERIALS AND METHODS

The original starter cultures of WI-38 and WI-38 VA13A were obtained from Dr. Paul F. Kruse, Jr. and Dr. V. J. Cristofalo, respectively. Both cell types were cultured in basal medium (Eagle), BME, containing Earle's salts, 10% calf serum, 100 units of penicillin per ml of medium and 100 mcg of streptomycin per ml of medium. One liter of medium was prepared by adding 100 ml of 10 X BME with Earle's salts, 20 ml of a solution containing 5,000 mcg of streptomycin and 5,000 units of penicillin per ml, 100 ml of calf serum, and 50 ml of a sterile solution (sterilized with a Millipore stainless steel pressure filter holder using compressed nitrogen at a pressure head of 5 psi) of 4.4% (w/v) sodium bicarbonate to 730 ml of water. The water was double distilled in a glass still and sterilized for 45 minutes by double autoclaving at a 24 hour interval. All 10 X BME, antibiotics, and calf serum were purchased from Grand Island Biological Company.

Both cell types were grown in two liter Povitsky flasks with 150 ml of complete medium. The bottles were

gassed through tightly cotton packed 25 ml pipettes for 30 seconds with a 5% CO<sub>2</sub> in air mixture and then stoppered with silicone stoppers (West and Company). Prior to use, the Povitsky flasks were soaked in 7X soap (Linbro Chemical Company) for at least one week and then vigorously rinsed with tap water, followed by a rinse with double glass distilled water. When the pH of the medium fell to about seven, the medium was changed and the flask restoppered without gassing. After the pH of the second feeding dropped to about seven, the medium was removed; and the cells were ready to be harvested.

The cell sheet was harvested from the glass surface by treatment with an 0.05% (w/v) pronase solution. The pronase was purchased from Calbiochem. The pronase solution was prepared by adding 50 mg of pronase per 100 ml of Earle's salt solution minus glucose and was sterilized by filtration through a candle type sterilizing filter. To each two liter Povitsky flask, 10 ml of sterile pronase solution was added. The pronase was left in contact with the cell sheet until the cell sheet began to form a mosaic-like pattern, and then the pronase solution was rapidly decanted before the cell sheet could break loose from the surface on which it was growing. After removing the pronase the flask was agitated by rocking until the cell sheet was completely free from the surface. Then 10 ml of medium was added to the cells and was aspirated vigorously at least ten times to

break up cell clumps. This was accomplished with a sterile cotton plugged 10 ml plastic pipette (Falcon Plastics). For WI-38 all but 3 ml of the aspirated cell-medium solution was removed and added to a sterile centrifuge tube and for WI-38 VA13A all but one ml of cells and medium was removed and also added to a sterile centrifuge tube. The cells were centrifuged at 2500 rpm for 15 minutes and the pellet was used in various assays. To the cells remaining in the Povitsky flask 150 ml of medium was added, and the flask was gassed for 30 seconds with a 5% CO<sub>2</sub> in air mixture and stoppered with a silicone stopper. All harvesting and transfers were performed in a laminar flow clean working station (Agnew-Higgins, Inc.) and all glassware was washed in 7X soap before use.

For the glucose and lactate determinations the spent medium was removed and immediately deproteinated with an equal volume of 0.6M perchloric acid. The original inoculum of cells and the final number of cells were determined by diluting the cells to 300 to 400 cells per hemacytometer chamber with fresh medium and counting in duplicate. Usually, the proper dilution for the hemocytometer when using two liter Povitsky flasks is 1 to 5 for WI-38 and 1 to 10 for WI-38 VA13A. The concentration of glucose was determined by using a Sigma glucose determination kit. The instructions suggest that the blank contain 0.1 ml of color reagent (2.5 mg o-dianisidine dihydrochloride per ml),

6.0 ml enzyme solution which contains buffered glucose oxidase and peroxidase, and 0.2 ml of distilled water. Each assay on the spent medium was prepared as the blank except that 0.2 ml of deproteinized medium was substituted for the 0.2 ml of distilled water. The assays were made in triplicate with one blank. After the assay mixtures have incubated at 37°C for two hours, the change in absorbance was measured against the blank at 500 nm. The absorbance value was converted to concentration of glucose in the deproteinized medium in mg/ml by dividing it by 0.84. The 0.84 value is determined from a standard curve which was prepared by diluting the stock medium, which contains one mg of glucose per ml, with an Earle's salt solution to obtain the desired glucose concentration. Then each glucose solution was deproteinized with an equal volume of 0.6 M perchloric acid, centrifuged, and assayed as previously described. The mg of glucose consumed was calculated by subtracting the mg of glucose per ml in the spent medium from 1 mg per ml which is the original concentration of glucose in the fresh medium. After the mg of glucose consumed was determined, it was converted to micromicromoles per hour per cell change. For the determination of lactate a spectrophotometric procedure from a Calbiochem Biochemica Test Combination instruction sheet (art. no. 15972) was adapted to a 3 ml assay. The blank contained 2.5 ml of a 0.50 M glycine buffer which was made 0.40 M in hydrazine sulfate (Eastman

Kodak) and buffered to pH 9.0 by adjustment with sodium hydroxide; 0.2 ml of 0.027 M diphosphopyridinenucleotide; 0.2 ml of a lactic acid dehydrogenase solution (1 mg protein/ml); and 0.1 ml of the deproteinized fresh medium. The hydrazine in the buffer reacted with the pyruvate that was formed in order to prevent the reverse of the enzymic reaction. The assays were prepared in the same way as the blank except 0.1 ml of spent medium was substituted for 0.1 ml of the fresh medium. The assays were performed in triplicate with one blank. After thirty minutes of time at 37°C the absorbance of each assay was measured against the blank at 366 nm. Multiplication of the absorbance average by 1.9 converted it to mg of lactate produced per ml which was then converted to micromicromoles per hour per cell change. The standard curve was obtained by adding lactate to the medium and by deproteinizing the solution with an equal volume of 0.6 M perchloric acid before assaying.

For the preparation of a cell-free extract for the adenylate assays, the cell sheet was loosened by pronase treatment as previously described. To the free cell sheet 10 ml of medium was added per Povitsky flask, and the solution was aspirated at least ten times. Then an appropriate quantity of aspirated solution was transferred to a 25 ml graduated cylinder, and the solution was titered with fresh medium to a volume that was readily divisible by three. An aliquot of cells was removed, diluted to 300 to 400 cells

per hemocytometer, and counted in duplicate. The medium-cell suspension was dispensed while thoroughly dispersed so that one centrifuge tube contained two-thirds of the cells and the other centrifuge tube contained one-third of the cells, and both cell solutions were centrifuged at 3,000 rpm for 15 minutes. The pellet which contained two-thirds of the cells was suspended in 50 ml of 0.16 M succinate buffer which had been adjusted to a pH of 6.1 with sodium hydroxide. The other pellet containing one-third of the cells was suspended in 25 ml of 0.10 M tris - HCl buffer at pH 7.5. Both buffers were preheated to 60°C before adding to the cells in order to denature any enzymes that might alter the levels of adenine nucleotides after the cells had been broken. While the cells were maintained at 60°C, they were sonicated at least 120 seconds at maximum cavitation. The temperature of the buffers was held at 60°C for a total of four minutes, and then the sonicate was cooled rapidly to 0°C by transferring to a precooled centrifuge tube (-20°C) and by swirling the tube containing the sonicate in a salt-ice-water bath. The cooled sonicate was centrifuged at 15,000 rpm for 20 minutes at 0°C, and the appropriate quantity of the supernatant was used for estimating the levels of adenylates in each cell type. The sonicates that were prepared in the succinate buffer were used to determine adenosine monophosphate (AMP) and adenosine diphosphate

(ADP) levels, and the sonicate prepared in the tris buffer was used to determine adenosine triphosphate (ATP) levels.

The procedures used to determine AMP and ADP were adopted from Kalckar's procedures (33). For AMP determination the blank contained 1.0 ml of the succinate buffer and 2.0 ml of assay solution which was the supernatant of the centrifuged sonicate. Assays were run in triplicate and contained 1.0 ml of 5'-adenylic acid deaminase solution (0.08 micromolar units per ml of succinate buffer) and 2.0 ml of assay solution. Since the absorption of the assay solution was significantly greater than a correction blank containing 2.0 ml succinate buffer and 1.0 ml of assay enzyme, the AMP was determined directly from the difference in absorption of the blank and assay. The difference in absorbance was read at 265 nm after 45 minutes incubation at room temperature, and it was multiplied by 0.294 to give the concentration of AMP in the assay solution in micromoles per ml. Measurement of ADP was performed in an analogous manner. The blank that was used in the ADP determinations was identical to the blank prepared for the AMP determination. As in the AMP determination a correction blank containing the assay enzymes was not necessary. The ADP level was measured in a three ml assay containing 0.16 micromolar units of 5'-adenylic acid deaminase, and 10 micromolar units of myokinase in 1.0 ml of succinate buffer and 2.0 ml of assay solution. The difference in absorbance was read at

265 nm after 60 minutes incubation at room temperature.

Since the ADP assay measured both the AMP present in the solution and the AMP produced via the myokinase catalyzed reaction, the absorption of the ADP assay must be corrected for endogenous AMP by subtracting the absorbance of the AMP assay from the total absorption of the ADP assay. Thus the difference in the absorbance between the ADP and AMP assays is multiplied by 0.130 to obtain the concentration of ADP in micromoles per ml of assay solution. The empirical factor 0.130 was obtained from a standard curve.

The procedure used to determine the ATP levels was adapted from the method developed by Kornberg (35). The blank contained 1.0 ml of 0.10 M tris-HCl buffer at a pH of 7.5 and 2.0 ml of the tris assay solution. However, in contrast to the AMP and ADP assays a correction blank must be used for the ATP determination. The correction blank contained 2.0 ml of tris buffer; 0.2 of a .15 M glucose solution; 0.2 ml of a 15 mM  $MgCl_2$  solution; 0.2 ml of a 1.5 mM triphosphopyridine nucleotide solution; 0.2 ml of a hexokinase solution containing 9 U. per ml of tris; and 0.2 ml of a glucose-6-phosphate dehydrogenase solution (0.06 mg protein per ml). The assay differed from the correction blank in that 2.0 ml of tris assay solution replaced the 2.0 ml of tris buffer. Since the absorbance measured for the ATP assay was not an equilibrium value, the absorbance must be read after 20 minutes incubation and no later than



25 minutes incubation time. Thus the change in absorbance was read as rapidly as possible after 20 minutes at 340 nm for both the assay and the correction blank. By subtracting the absorbance of the correction blank from the absorbance of the assay, a corrected absorbance was obtained. By multiplying the corrected absorbance by 0.326 the  $\mu$ moles of ATP per ml of tris assay solution was obtained. The standard curve was prepared by incubating the ATP standards for 20 minutes only and the factor 0.326 was determined from this curve. All adenine nucleotide levels were converted to millimicromoles per  $10^6$  cells for tabulation. All assay enzymes, substrates, and cofactors were purchased from Sigma Chemical Company unless otherwise specified.

For determination of the enzyme patterns in WI-38 and WI-38 VA13A it was found that the procedures outlined by Shonk and Boxer for human tissues were readily adaptable to the determination of enzyme patterns in human tissue grown "in vitro" (50). The basic methodology that they used for the determination of the glycolytic enzymes depends on the coupling of the enzyme whose rate was to be measured to the oxidation and reduction of the pyridine nucleotides. The rate of appearance of product was equated to rate of appearance or disappearance of reduced pyridine nucleotides directly or indirectly by coupled assays. By converting the change in absorbance to change in micromoles of reduced pyridine nucleotide, the micromoles of product formed is

estimated. It was found that by multiplying the change in absorbance at 340 nm by 0.482 that the micromoles of reduced pyridine nucleotide consumed or formed in a 3 ml assay using 1 cm cuvettes can be calculated, and this was equated directly with the micromoles of product formed by the enzyme whose activity was to be measured (27).

For the enzyme pattern studies the cells were pelleted as described in the second and third paragraphs of this chapter. The cell pellet was suspended in 5 ml of precooled extraction medium by aspiration and transferred to a precooled sonication tube. The extraction medium which was prepared in glass double distilled water contained potassium chloride, 0.15M; potassium bicarbonate, 0.05M; and disodium ethylenediaminetetracetic acid, 0.006M. The cells were sonicated two minutes at maximum cavitation using a probe that had been precooled to  $-20^{\circ}\text{C}$ . When the sonication tube began to feel warm to the touch, it was immersed in a salt-ice-water bath to rapidly cool the surface of the tube. The sonicate was transferred to a Nalgene centrifuge tube that had been precooled to  $-20^{\circ}\text{C}$ , and then the tube was immersed into a salt-ice-water bath and agitated until the temperature of the sonicate was about  $0^{\circ}\text{C}$ . The precooled sonicate was centrifuged at 15,000 rpm for 30 minutes in a Sorval RC-2B centrifuge with a SS-34 head at  $0^{\circ}\text{C}$ . The supernatant was used directly to assay the desired enzymes and immediately for determination of enzyme patterns.

Each enzyme was measured in tris buffer (0.05 M) at pH 7.6 containing disodium ethylenediaminetetracetic acid (0.006 M). All substrates, cofactors, and assay enzymes were purchased from Sigma Chemical Company and used directly without further purification. None of the assay enzyme solutions were dialyzed, and all assay enzyme solutions were prepared daily. All substrates and cofactors were prepared on a weekly basis. Each assay was started with the supernatant and was determined in duplicate at room temperature ( $25 \pm 1^{\circ}\text{C}$ ). A blank was measured for each of the assay conditions, and it was found that the activity of the blank ceased in two to five minutes. Sonication of the cells longer than two minutes significantly increases the oxidation of reduced pyridine nucleotides and, thus, it was a necessity not to sonicate longer than two minutes.

The following paragraph lists the millimoles (mM) of reagents added to a 3 ml assay, and the activity of the assay enzymes is given in units (U). One unit (U) of any enzyme is defined as "that amount of enzyme which will catalyze the transformation of one micromole of substrate per minute (17)."

1. Glyceraldehyde Phosphate Dehydrogenase (GAPDH)

- a. 12 mM Sodium Arsenate
- b. 0.4 mM Diphosphopyridine Nucleotide ( $\text{NAD}^{+}$ )
- c. 0.6 mM L Glyceraldehyde-3-Phosphate (GAP)

## 2. Pyruvate Kinase (PK)

- a. 10 mM  $\text{MgCl}_2$
- b. 0.3 mM Reduced Diphosphopyridine Nucleotide (NADH)
- c. 3.0 mM Phosphoenol Pyruvate (PEP)
- d. 3.0 mM Adenosine Diphosphate (ADP)
- e. 9.1 U Lactic Acid Dehydrogenase
- f. Time must be allowed for any pyruvate in the phosphoenol pyruvate to be consumed

## 3. Phosphofructokinase (PFK)

- a. 10 mM  $\text{MgCl}_2$
- b. 0.3 mM NADH
- c. 3.0 mM Adenosine Triphosphate (ATP)
- d. 3.0 mM Fructose-6-Phosphate (F-6-P)
- e. 1.0 U Aldolase
- f. 7.1 U  $\alpha$ -glycerol phosphate dehydrogenase
- g. 18.3 U Triosephosphate Isomerase
- h. Since two moles of NADH are oxidized per mole of substrate utilized, the observed rate has to be divided by two to express the measurement in U

## 4. Phosphoglycerate Kinase (PGK)

- a. 10 mM  $\text{MgCl}_2$
- b. 0.3 mM NADH
- c. 2.8 mM Cysteine
- d. 2.8 mM 3-Phosphoglyceric Acid (3PGA)
- e. 2.8 mM ATP
- f. 4.3 U GAPDH

5. Hexokinase (HK)
  - a. 10 mM  $\text{MgCl}_2$
  - b. 0.35 mM Triphosphopyridine Nucleotide ( $\text{NADP}^+$ )
  - c. 2.8 mM Glucose
  - d. 2.8 mM ATP
  - e. 4.3 U Glucose-6-Phosphate Dehydrogenase
6. Glucose-6-Phosphate Dehydrogenase (GPDH)
  - a. 10 mM  $\text{MgCl}_2$
  - b. 0.36 mM  $\text{NADP}^+$
  - c. 3.0 mM Glucose-6-Phosphate (G-6-P)
7. 6-Phosphogluconate Dehydrogenase (6PGADH)
  - a. 10 mM  $\text{MgCl}_2$
  - b. 0.36 mM  $\text{NADP}^+$
  - c. 3.0 mM 6-Phosphogluconic Acid
8. Phosphoglucomutase (PGM)
  - a. 20 mM  $\text{MgCl}_2$
  - b. 0.36 mM  $\text{NADP}^+$
  - c. 3.0 mM Glucose-1-Phosphate
  - d. 4.3 U GPDH
  - e. Evidently, glucose-1,6-diphosphate was present in adequate catalytic amounts
9. Lactate Dehydrogenase (LDH)
  - a. 0.3 mM NADH
  - b. 6.2 mM Pyruvate (Pyr)

## 10. Aldolase

- a. 0.3 mM NADH
- b. 3.0 mM Fructose-1,6-Diphosphate
- c. 7.1 U Glycerolphosphate Dehydrogenase
- d. 18.3 U Triosephosphate Isomerase
- e. The observed rate is divided by two (see PFK)

## 11. Phosphoglucoisomerase (PGI)

- a. 10 mM  $\text{MgCl}_2$
- b. 0.36 mM  $\text{NADP}^+$
- c. 3.0 mM Fructose-6-Phosphate
- d. 4.3 U GPDH
- e. All of the G-6-P which contaminates the F-6-P is consumed within one minute

## 12. Fructosediphosphatase (FDPase)

- a. 10 mM  $\text{MgCl}_2$
- b. 0.36 mM  $\text{NADP}^+$
- c. 3.0 mM Fructose-1,6-Diphosphate
- d. 4.3 U GPDH

Three of the enzymes that showed a statistical variation in their specific activities (expressed as millimicro-moles of substrate utilized per minute per  $10^6$  cells) for the two cell types and one that was not a statistical variant were selected for a more detailed kinetic study. For each of the enzymes in both sources, a pH profile, saturation curve, Hill plot (3), and Lineweaver-Burk plot (40) were determined. The pH profile was accomplished in all cases

by using 50 mM tris buffers at pHs of 7.00, 7.25, 7.50, 7.75, 8.00, 8.50, 9.00, and 9.50 and 50 mM imidazole buffers at pHs of 6.0, 6.5, 7.0 and 7.5. The pH of each buffer was adjusted immediately before using with the expanded scale of a Corning pH meter. Each assay had concentrations of substrates and cofactors as previously described, i.e.  $V_m$  conditions. The data for the saturation curves, Hill plots, and Lineweaver-Burk plots were determined for each substrate by varying one substrate so that the lowest reaction rate was at least  $0.1 V_m$  while the other substrates were maintained at enzyme saturating levels.

Also for the same four enzymes many of the glycolytic and tricarboxylic acid cycle intermediates were examined as possible effectors of enzymic rate. Since some of these compounds were capable of chelating magnesium ions, 20 millimoles of  $MgCl_2$  was added to a 3.0 ml assay. All of these compounds were purchased from Sigma Chemical Company.

## CHAPTER IV

### EXPERIMENTAL RESULTS

In Table 1 is presented the glucose consumption and lactate production by WI-38 and WI-38 VA13A. Four individual experiments were run and the average of triplicate determinations is recorded in Table 1. The average and standard deviations were determined using an Olivetti Underwood Programma 101 Electronic Desk Computer. The standard deviation was computed by the formula,  $s = (\sum (\bar{x} - x) / n - 1)^{1/2}$  using a program card generously donated by Mr. Phillip Schafer.

TABLE 1.--Glucose consumption and lactate production in WI-38 and WI-38 VA13A. All values are expressed in micromicromoles per cell change per hour.  
s is the standard deviation

Attempt	Glucose Consumed		Lactate Produced	
	WI-38	WI-38 VA13A	WI-38	WI-38 VA13A
1	1.88	0.73	4.10	1.49
2	1.99	0.83	3.46	1.45
3	2.09	0.86	3.33	1.43
4	1.60	0.69	4.02	0.96
Avg. $\pm$ s	1.89 $\pm$ .21	0.78 $\pm$ .08	3.78 $\pm$ .39	1.33 $\pm$ .24



Based on Table 1 several conclusions can be made by comparing the glucose consumption and lactate production of WI-38 and WI-38 VA13A. Since the ratio of lactate production to glucose consumption is approximately 2.0 and 1.7 for WI-38 and WI-38 VA13A, respectively, it is concluded that the predominate fate of glucose is lactate formation. Also the lactate production is about 2.7 fold greater in WI-38, and glucose consumption is about 2.4 fold greater in WI-38.

Located in Tables 2-A and 2-B are the concentrations of each adenine nucleotide in WI-38 VA13A and WI-38, respectively. Each value is the average of triplicate determinations with  $s$  being calculated as previously described.

TABLE 2-A.--Levels of adenine nucleotides in WI-38 VA13A.  
The levels are reported in millimicromoles per  $10^6$  cells.  $s$  is the standard deviation

Attempt	ATP	ADP	AMP
1	18.6	11.1	40.8
2	16.6	11.5	45.3
3	15.0	10.5	33.4
4	16.7	11.9	40.1
Avg. $\pm s$	16.7 $\pm$ 1.5	11.3 $\pm$ 0.6	39.9 $\pm$ 4.9

TABLE 2-B.--Levels of adenine nucleotides in WI-38. The levels are reported in millimicromoles per  $10^6$  cells. s is the standard deviation

Attempt	ATP	ADP	AMP
1	7.0	19.5	84.8
2	5.1	15.8	68.4
3	10.1	17.1	78.0
4	8.4	18.0	69.2
Avg. $\pm$ s	7.7 $\pm$ 2.1	17.6 $\pm$ 1.6	75.1 $\pm$ 7.8

By comparison it is evident that ATP levels in WI-38 are about 2 fold less than the ATP levels found for WI-38 VA13A. However, the AMP level is nearly 2 fold greater in WI-38 and the ADP level is about 1.5 times as large as in WI-38. The total concentrations of adenine nucleotides for each cell type indicates that WI-38 adenine nucleotide pool is nearly 1.5 fold larger than the WI-38 VA13A adenine nucleotide pool. Furthermore when the percent concentration of each adenine nucleotide in the estimated pool is calculated, the following results are obtained for WI-38: 7.7% ATP, 17.5% ADP, and 74.8% AMP and for WI-38 VA13A: 24.8% ATP, 16.7% ADP and 58.5% AMP. Thus when expressed on the basis of percent of the total adenine nucleotide pool the percent ADP is nearly the same for both sources, but the ATP and AMP levels are significantly different.

Tables 3-A and 3-B show the enzyme patterns for WI-38 and WI-38 VA13A, respectively. Each value is the

average of duplicate determinations and is calculated from the eight individual values by the manner previously described. From Tables 3-A and 3-B it is discernible that all of the glycolytic enzymes except enolase and phosphoglyceromutase were measured for both cell types as well as GPDH and 6PGADH of the phosphogluconate oxidative pathway and the gluconeogenic enzymes PGM and FDPase. It is apparent from Tables 3-A and 3-B that FDPase is the enzyme of lowest activity in both sources. The low activity glycolytic enzymes are HK, PFK, and aldolase in both cell types. Comparison of Tables 3-A and 3-B show that both of the phosphogluconate oxidative pathway enzymes have a larger specific activity in WI-38 i.e. 2.1 and 1.6 fold greater specific activities of GPDH and 6PGADH, respectively. Also the glycolytic enzymes HK, PGI, and GAPDH are statistically different in the two cell types. HK is about 2.4 fold greater in WI-38, and GAPDH is about 2.1 greater in WI-38. However, the specific activity of PGI is about 1.3 fold higher in WI-38 VA13A. Also the gluconeogenic enzyme FDPase, is approximately 3 fold greater in WI-38.

Since HK, GPDH, and GAPDH differed statistically in their specific activities for both cell types and PK was thought to be highly regulated in human cells, they were selected for further analysis. These enzymes were studied by determining their pH profiles and saturation curves. From the compiled data for the saturation curves,

<u>Enzyme</u>	1	2	3	4	5	6	7	8	Avg $\pm$ $\sigma$
Glucose-6-Phosphate Dehydrogenase	63.1	73.7	74.2	57.8	62.7	60.0	58.8	61.7	64.0 $\pm$ 6.5
6-Phosphogluconate Dehydrogenase	8.7	9.2	9.6	7.2	7.7	7.7	8.7	6.8	8.2 $\pm$ 1.0
Phosphoglucomutase	4.3	3.7	3.1	4.3	5.3	3.1	3.9	3.6	3.9 $\pm$ 0.7
Hexokinase	12.5	15.4	14.5	13.5	11.1	12.1	14.0	10.6	13.0 $\pm$ 1.7
Phosphoglucoisomerase	247	210	212	222	298	323	242	266	253 $\pm$ 41
Phosphofructokinase	11.8	8.9	8.4	9.2	11.6	11.1	10.8	9.4	10.2 $\pm$ 1.3
Fructose Diphosphatase	0.96	1.06	2.51	1.54	1.40	1.49	2.07	1.35	1.55 $\pm$ 0.51
Aldolase	11.5	10.5	13.5	11.1	8.5	11.5	12.5	10.5	11.2 $\pm$ 1.5
Glyceraldehydephosphate Dehydrogenase	71.3	72.8	75.2	71.8	58.8	81.9	68.9	79.5	72.5 $\pm$ 7.0
Phosphoglycerate Kinase	242	246	269	274	350	376	286	246	286 $\pm$ 50
Pyruvate Kinase	252	252	234	198	252	209	215	220	229 $\pm$ 22
Lactate Dehydrogenase	240	251	245	225	326	284	336	242	269 $\pm$ 41

Table 3-A: Enzyme patterns in WI-38. Enzyme activities expressed in millimicromoles of substrate utilized per minute per  $10^6$  cells.  $\sigma$  is the standard deviation.

<u>Enzyme</u>	1	2	3	4	5	6	7	8	Avg $\pm$ $\sigma$	
Glucose-6-Phosphate Dehydrogenase	31.3	33.3	30.4	30.3	32.3	29.4	30.4	30.4	30.9 $\pm$ 1.4	
6-Phosphogluconate Dehydrogenase	4.8	5.8	5.7	4.4	4.4	5.2	5.7	4.8	5.1 $\pm$ 0.6	
Phosphoglucomutase	3.0	4.2	2.7	3.6	2.2	3.4	4.6	3.9	3.5 $\pm$ 0.8	
Hexokinase	5.8	4.8	4.8	5.8	6.3	5.8	6.3	4.8	5.5 $\pm$ 0.6	
Phosphoglucoisomerase	276	315	381	369	330	342	303	341	332 $\pm$ 32	
Phosphofructokinase	7.7	10.5	11.6	9.2	10.1	8.0	10.6	7.2	9.4 $\pm$ 1.6	
Fructose Diphosphatase	0.48	0.54	0.59	0.48	0.64	0.48	0.59	0.54	0.54 $\pm$ 0.06	30
Aldolase	16.1	16.4	15.9	13.0	16.7	14.2	12.1	14.9	14.1 $\pm$ 2.0	
Glyceraldehydophosphate Dehydrogenase	32.7	28.0	28.4	39.0	40.5	35.2	41.5	29.9	34.4 $\pm$ 5.5	
Phosphoglycerate Kinase	299	238	261	319	351	402	307	342	315 $\pm$ 52	
Pyruvate Kinase	256	242	250	240	271	256	265	249	254 $\pm$ 11	
Lactate Dehydrogenase	270	367	243	260	283	379	377	332	314 $\pm$ 56	

Table 3-B: Enzyme patterns in WI-38 VA13A. Enzyme activities expressed in millimicromoles of substrate utilized per minute per  $10^6$  cells.

Lineweaver-Burk plots (40) and Hill plots (3) were made, and these results are compared between the two sources in order to determine the extent of similarity between the various parameters.

From the Hill plots an interaction coefficient can be determined. The interaction coefficient is a reflection of the minimal number of substrate molecules that can be assumed to interact with an enzyme molecule. However, the interaction coefficient is only greater than one when the ligand binding shows cooperative interactions with other ligand binding sites, i.e. binding of each ligand affects further binding of another ligand. The interaction coefficient is a true measure of the order of the enzymic reaction only when binding site interactions occur and when the concentrations of any complexes containing fewer than  $n$  ligands is negligible compared to the  $ES_n$  complex. From the equation  $\log \frac{v}{V_m - v} = n \log (S) - \log K$ , where  $v$  is the reaction velocity at a substrate concentration of  $S$ ,  $V_m$  is the maximum attainable velocity, and  $n$  is the interaction coefficient, the interaction coefficient can be determined graphically. This is accomplished by plotting the values for  $\frac{v}{V_m - v}$  versus  $(S)$  on full logarithmic paper which results in the generation of a straight line whose slope is the interaction coefficient. Table 4 lists the interaction coefficients for the enzymes studied. When possible the values

for the reaction rates were selected between 0.1 and 0.9  $V_m$  for the Hill Plots.

TABLE 4.--A list of the Interaction Coefficients. Abbreviations may be found in Chapter III

Enzyme	Substrate	Interaction Coefficient For	
		WI-38	WI-38 VA13A
GPDH	G-6-P(< 0.045mM)	0.85,0.95	0.76,0.80
GPDH	G-6-P(> 0.45mM)	2.0,1.8	2.0,1.8
GPDH	NADP <sup>+</sup> (< 0.10mM)	0.84,0.75	0.90,0.88
GPDH	NADP <sup>+</sup> (> 0.10mM)	1.8,1.9	2.2,2.0
HK	ATP	0.96,1.0	0.87,0.95
HK	Glucose	1.0,1.0	0.98,1.0
GAPDH	GAP	1.5,1.4	1.5,1.5
GAPDH	NAD <sup>+</sup>	1.0,1.0,1.2	1.4,1.4,1.5
PK	PEP	1.8,2.0	1.8,2.0
PK	ADP	1.7,2.0	1.8,2.0

As can be seen from Table 4, the interaction coefficients for nearly all of the substrates are approximately identical for each enzyme regardless of the source. The only possible exception is the NAD<sup>+</sup> interaction coefficients for WI-38 and WI-38 VA13A. The NAD<sup>+</sup> interaction coefficient for WI-38 was always found in 3 independent determinations to be less than the one for WI-38 VA13A.

Table 5 is a tabulation of the optimum pH for each enzyme. All values were determined under substrate

saturating conditions using the buffers as described in Chapter III. The pH profiles for each enzyme from both cell types were nearly superimposable in all cases and the optimum pHs were identical in both types of cells. For HK two peaks of the pH profile were found, one at 7.7 and the other at 9.0. The peak at pH 9.0 was also the pH optimum for the assay enzyme GPDH, and it was found that at a pH of 9.0 the GPDH utilization of glucose was greater than at any other pH. Thus the NADPH production that was measured was the summation of utilization of the G-6-P produced by HK as well as the glucose present in the assay. By using a blank to measure glucose dehydrogenase activity of the assay enzyme at pH 9.0, it was found that pH 7.7 was the true pH optimum.

TABLE 5.--pH Optimum. Abbreviations may be found in Chapter III

Enzyme	pH Optimum for	
	WI-38	WI-38 VA13A
GPDH	8.0	8.0
HK	7.7 (9.0)	7.7 (9.0)
GAPDH	7.8	7.8
PK	7.2	7.2

In Figures 1 through 25, all saturation curves and Lineweaver-Burk plots are given for HK, GPDH, GAPDH, and PK for WI-38 and WI-38 VA13A. For GPDH in both cell types, the reciprocal values for concentrations of G-6-P greater



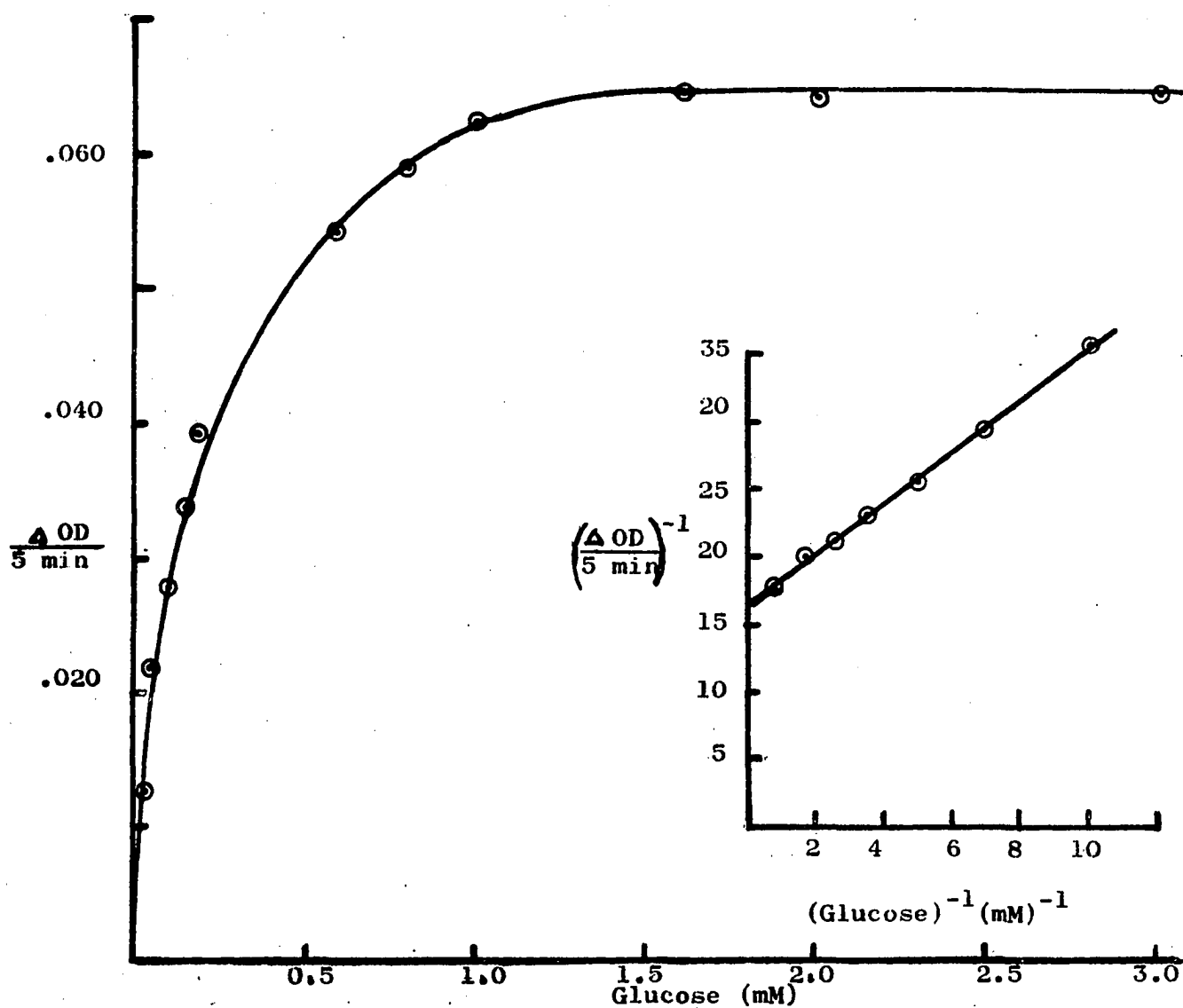


Figure 1: Glucose saturation of HK from WI-38 and corresponding Lineweaver-Burk Plot (inset). Abbreviations in Chapter III.

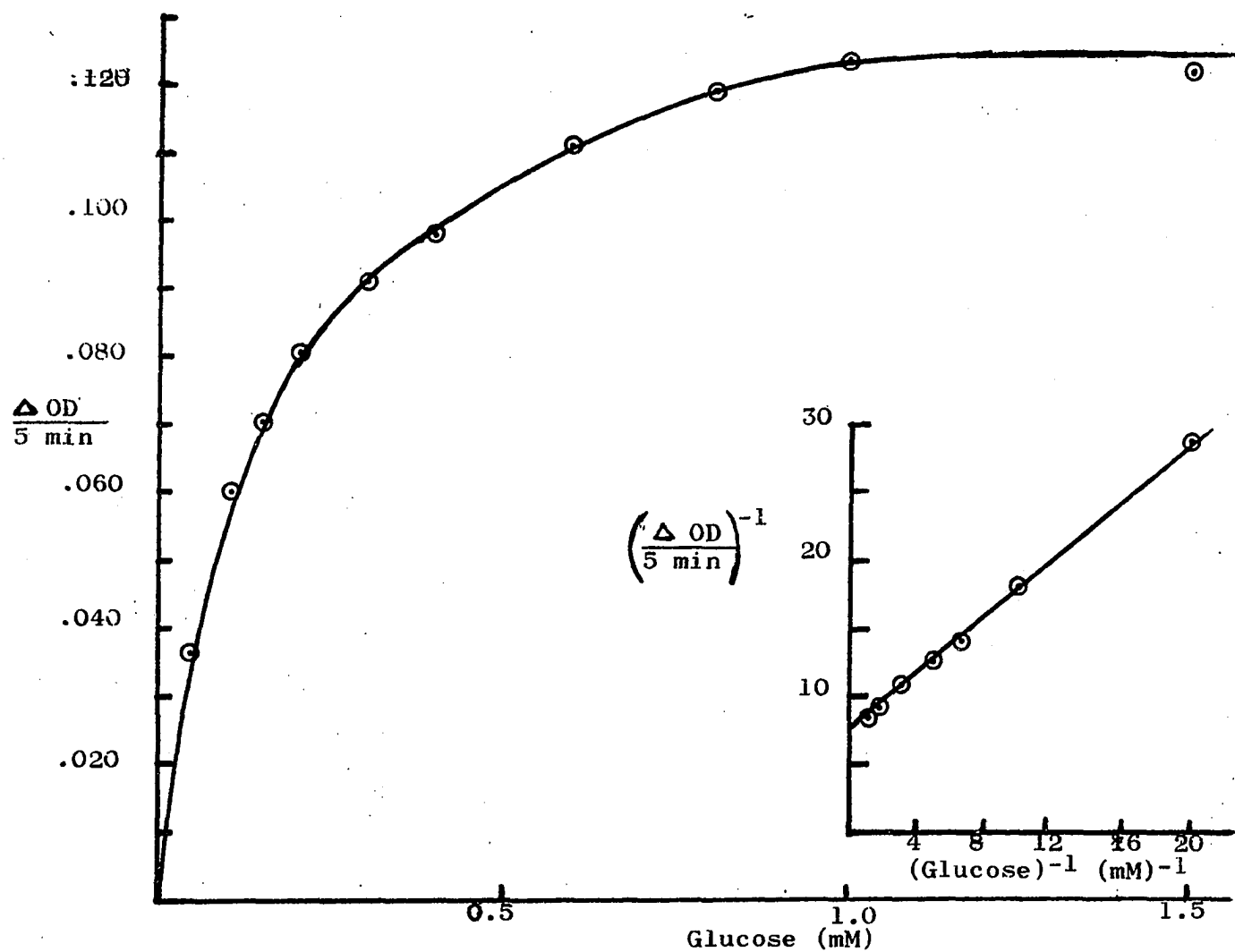


Figure 2: Glucose saturation of HK for WI-38 VA13A and corresponding Lineweaver-Burk Plot (insert). Abbreviations in Chapter III.

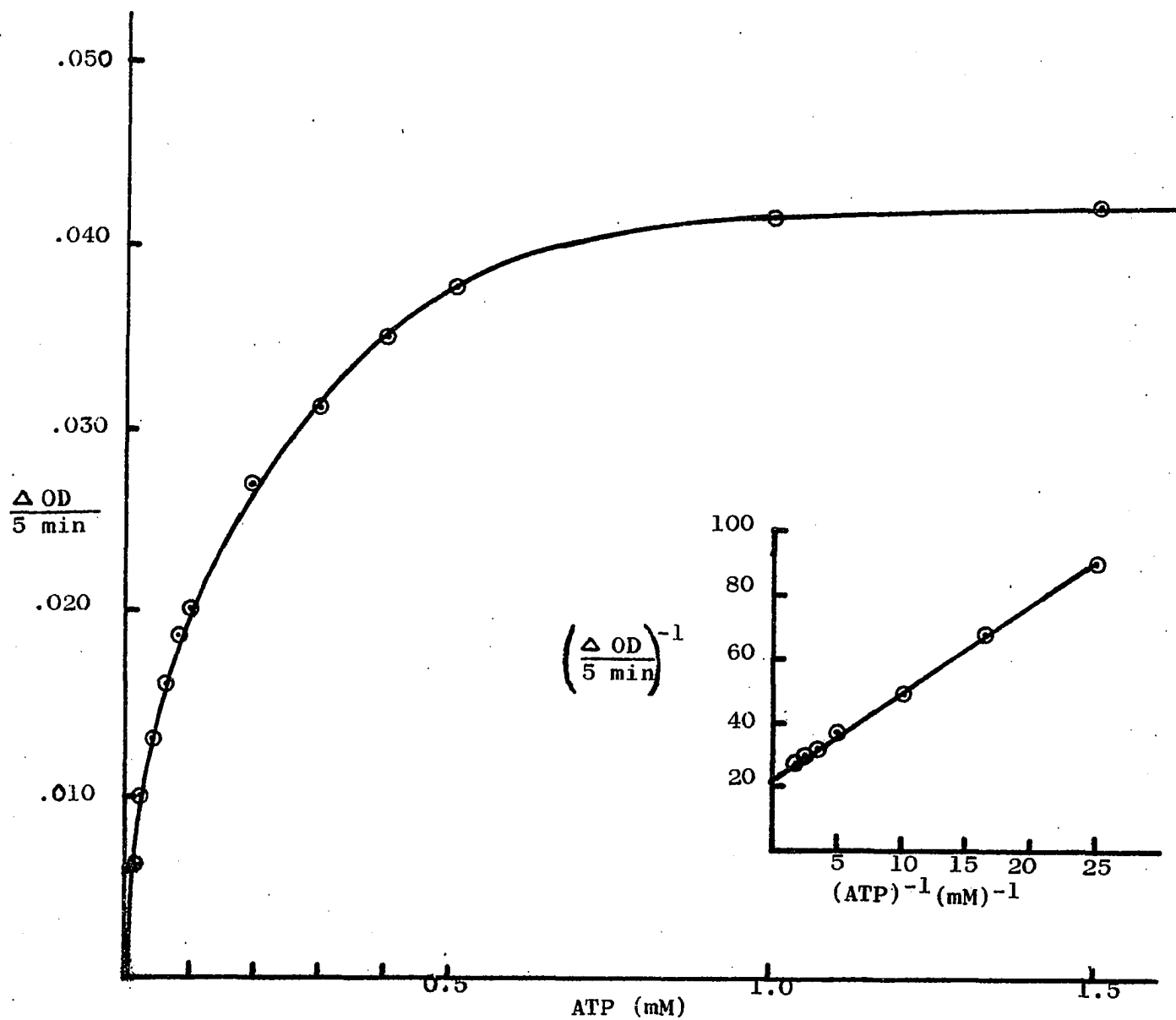


Figure 3: ATP saturation of HK from WI-38 and corresponding Lineweaver-Burk Plot (inset). Abbreviations in Chapter III.

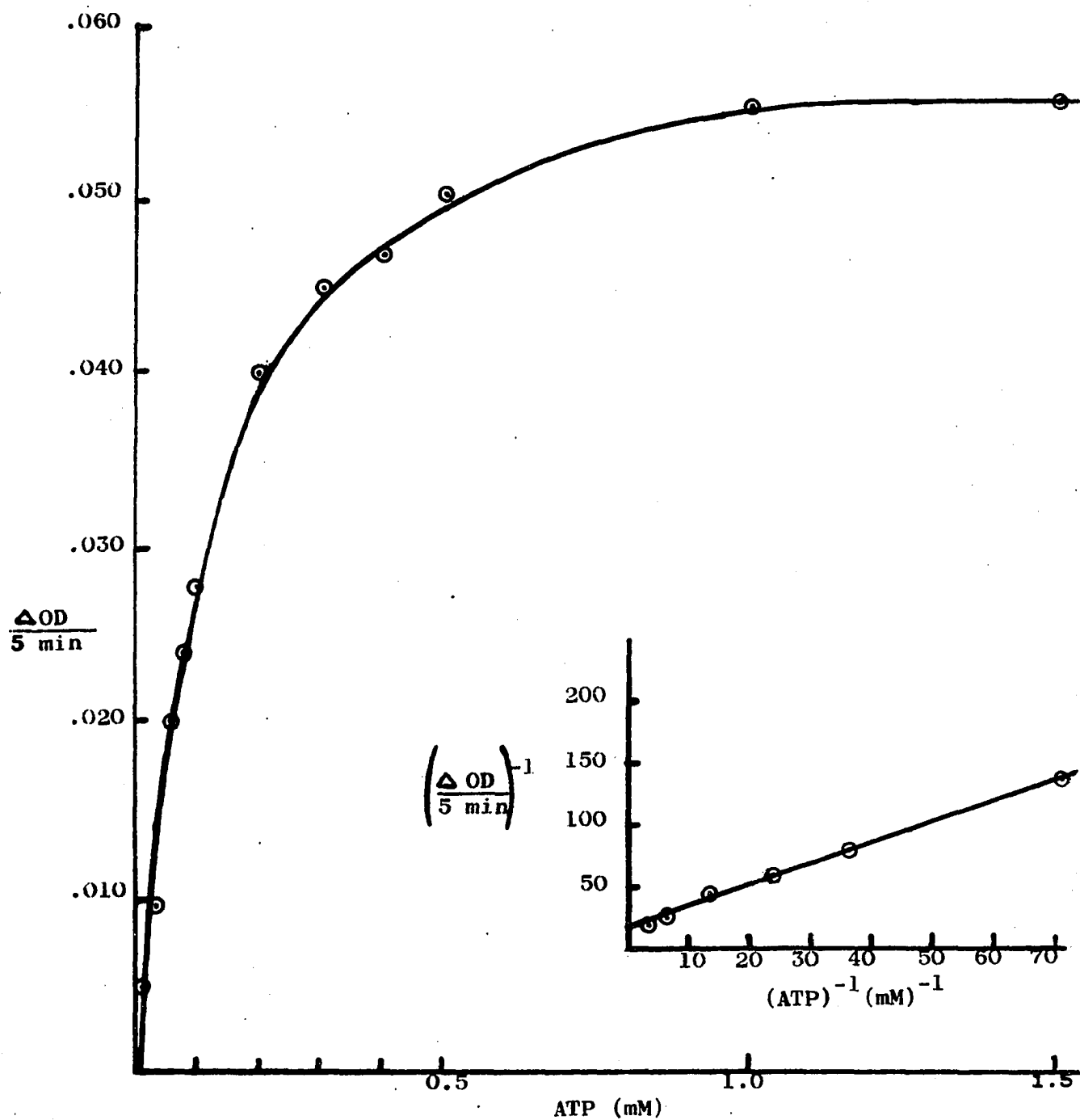


Figure 4: ATP saturation of HK from WI-38 VA13A and corresponding Lineweaver-Burk Plot (inset). Abbreviations in Chapter III.

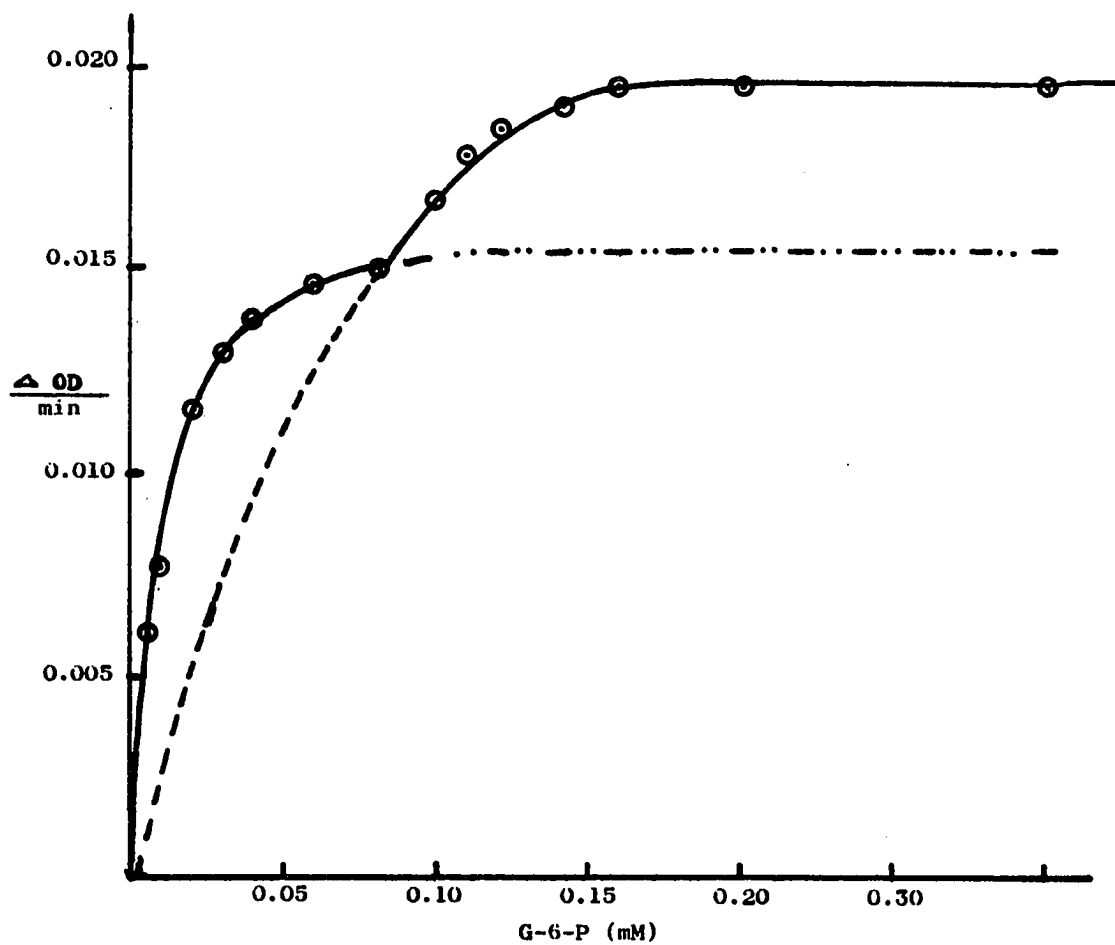


Figure 5: G-6-P saturation of GPDH from WI-38. Solid line is determined by experiment and dashed lines are extended to simulate overlapping saturation curves of two GPDH isozymes. Abbreviations found in Chapter III.

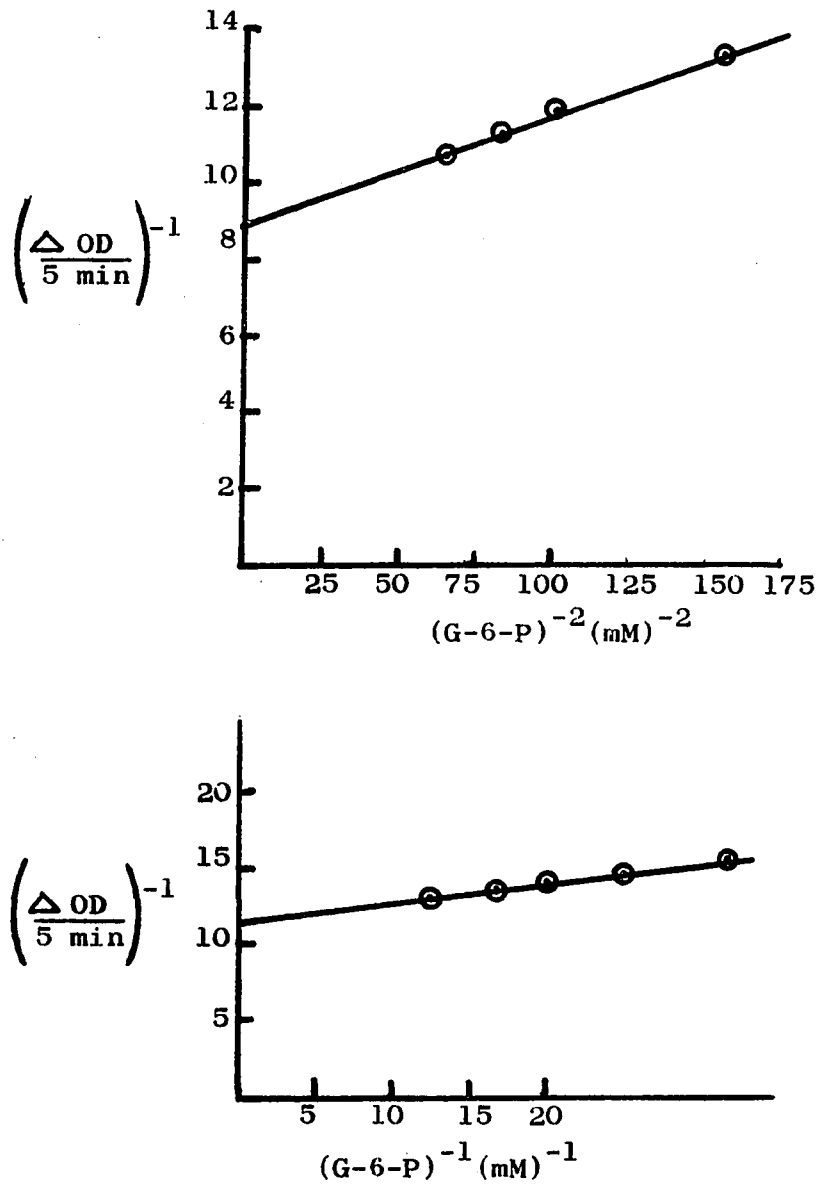


Figure 6: Lineweaver-Burk Plot of G-6-P saturation of WI-38 GPDH. G-6-P concentrations greater than 0.10 mM must be squared and are reported in top curve. G-6-P levels less than 0.10 mM are reported in lower curve. Abbreviations found in Chapter III.

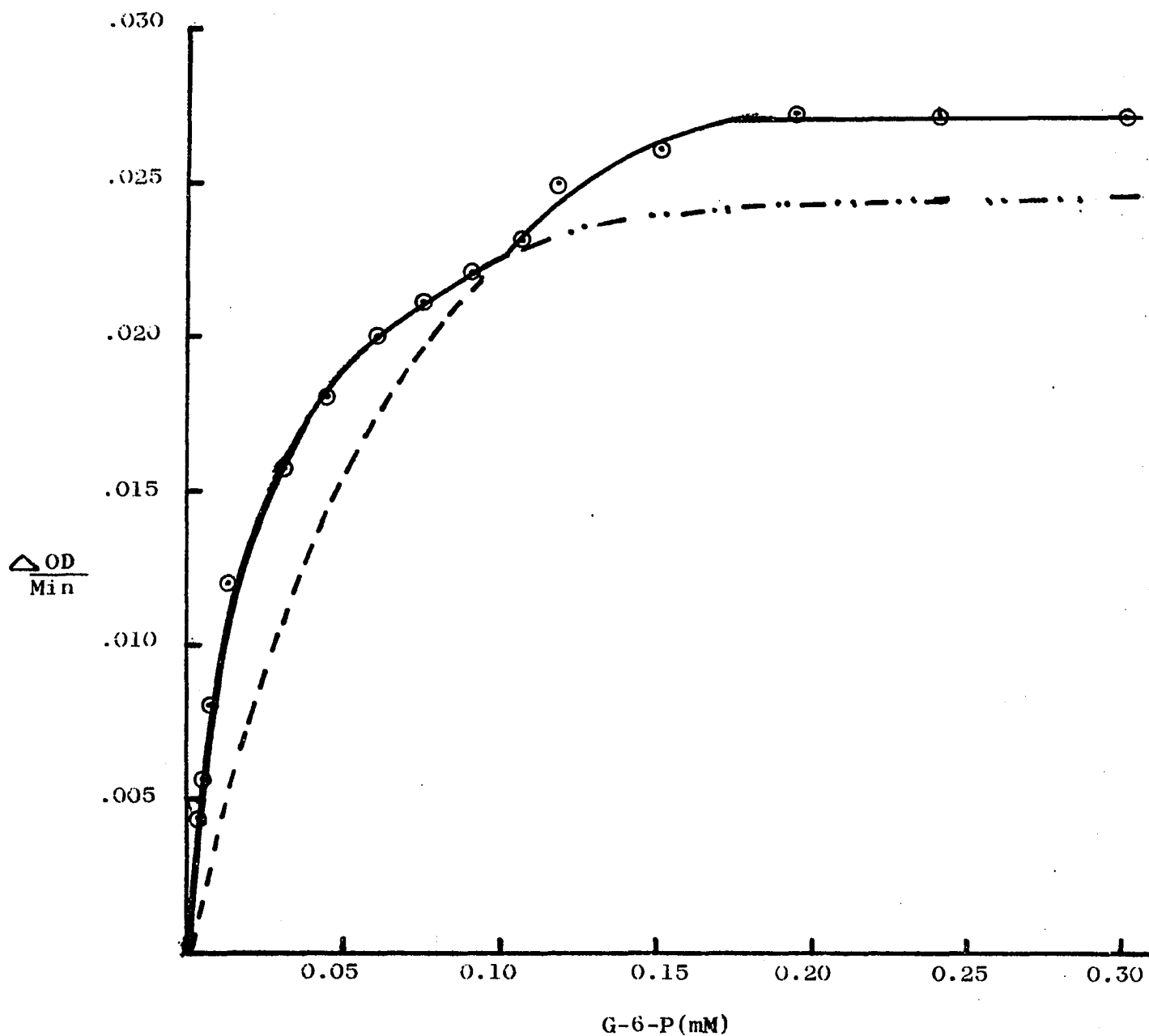


Figure 7: G-6-P saturation of GPDH from WI-38 VA13A. Solid line is determined by experiment, and dashed lines are extended to simulate overlapping saturation curves of two GPDH isozymes. Abbreviations found in Chapter III.

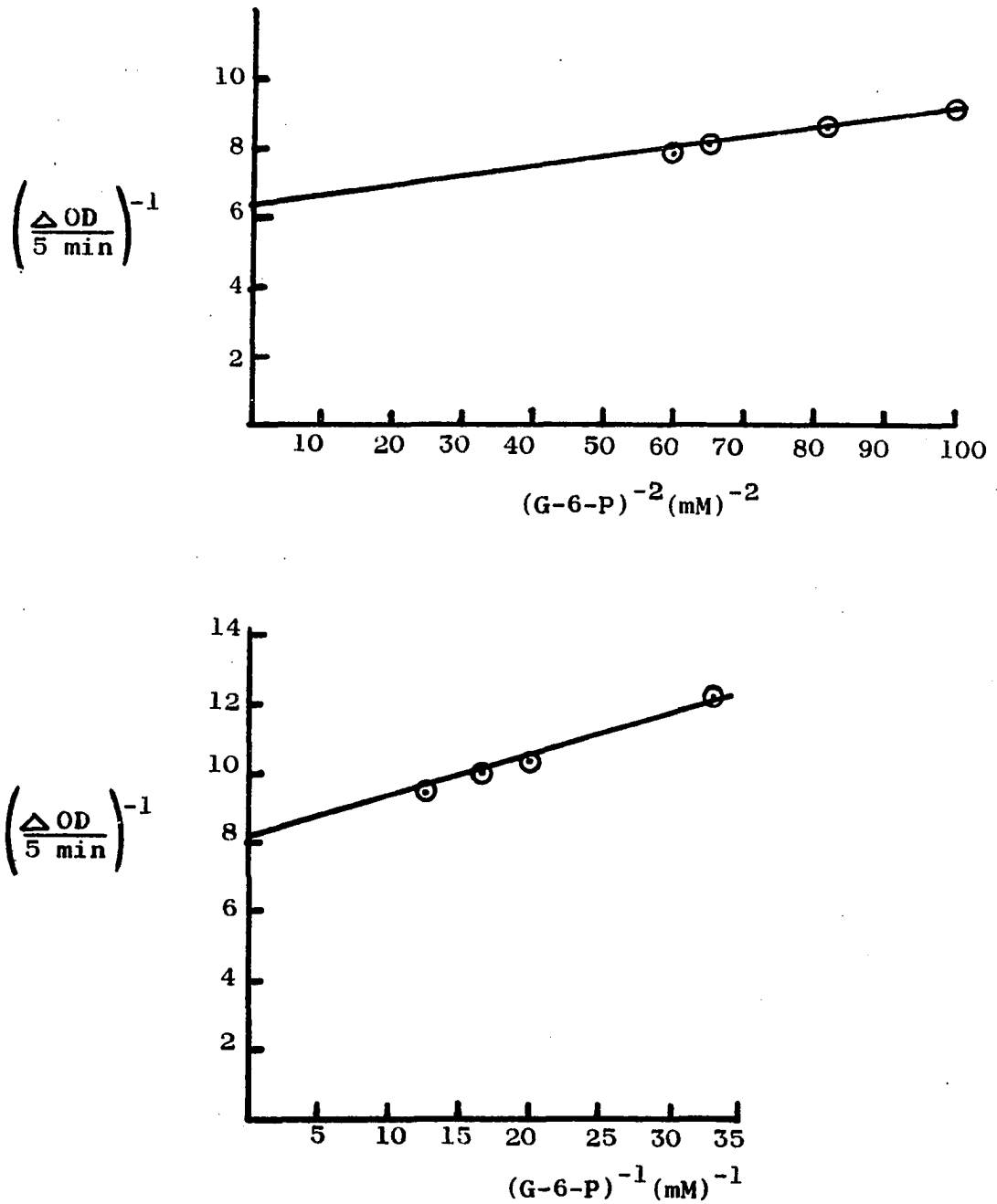


Figure 8: Lineweaver-Burk Plot of G-6-P saturation of WI-38 VA13A GPDH. G-6-P concentrations greater than 0.10 mM must be squared and are reported in top curve. G-6-P levels less than 0.10 mM are reported in lower curve. Abbreviations found in Chapter III.



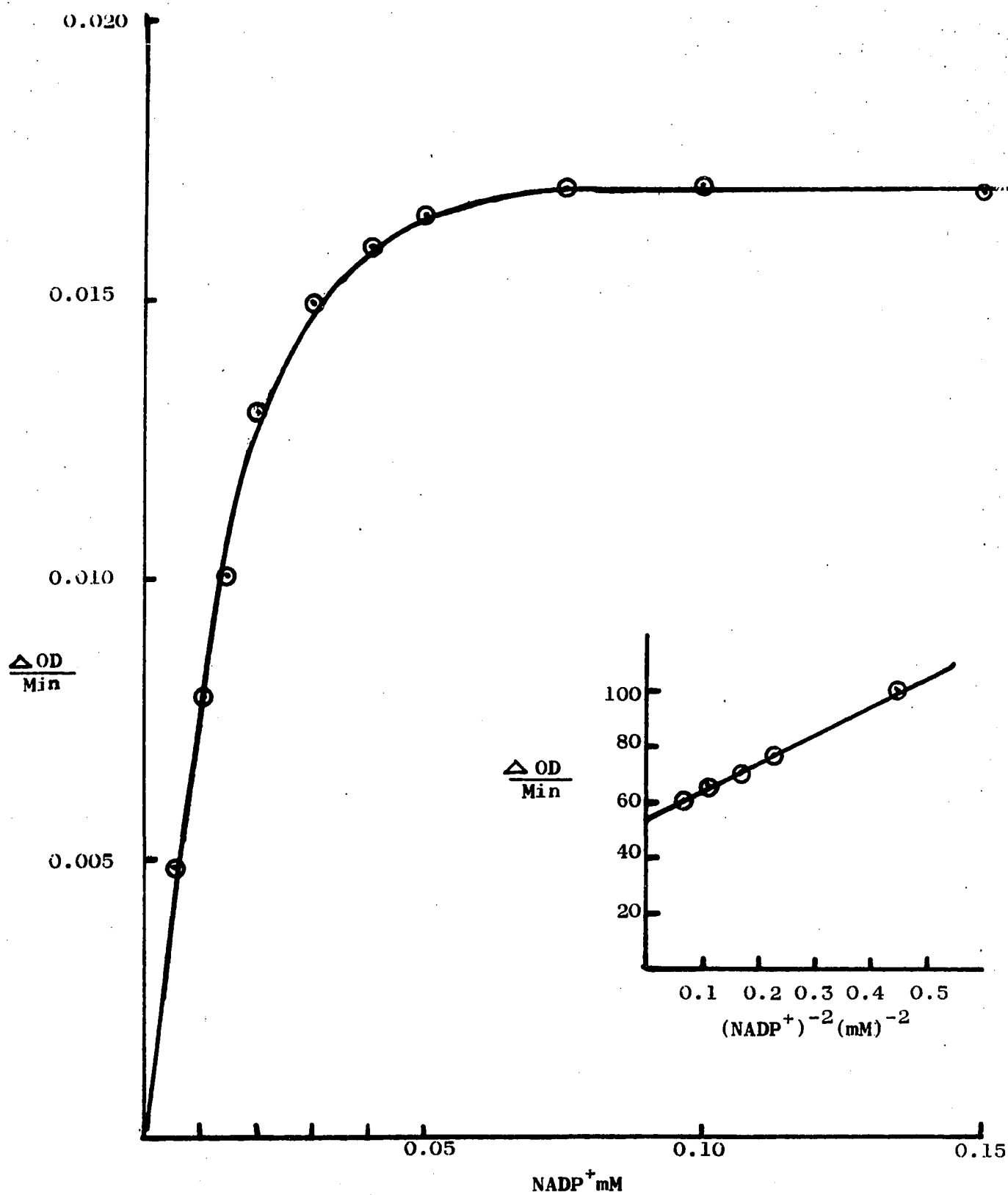


Figure 9: NADP<sup>+</sup> saturation of GPDH from WI-38. Abbreviations in Chapter III.

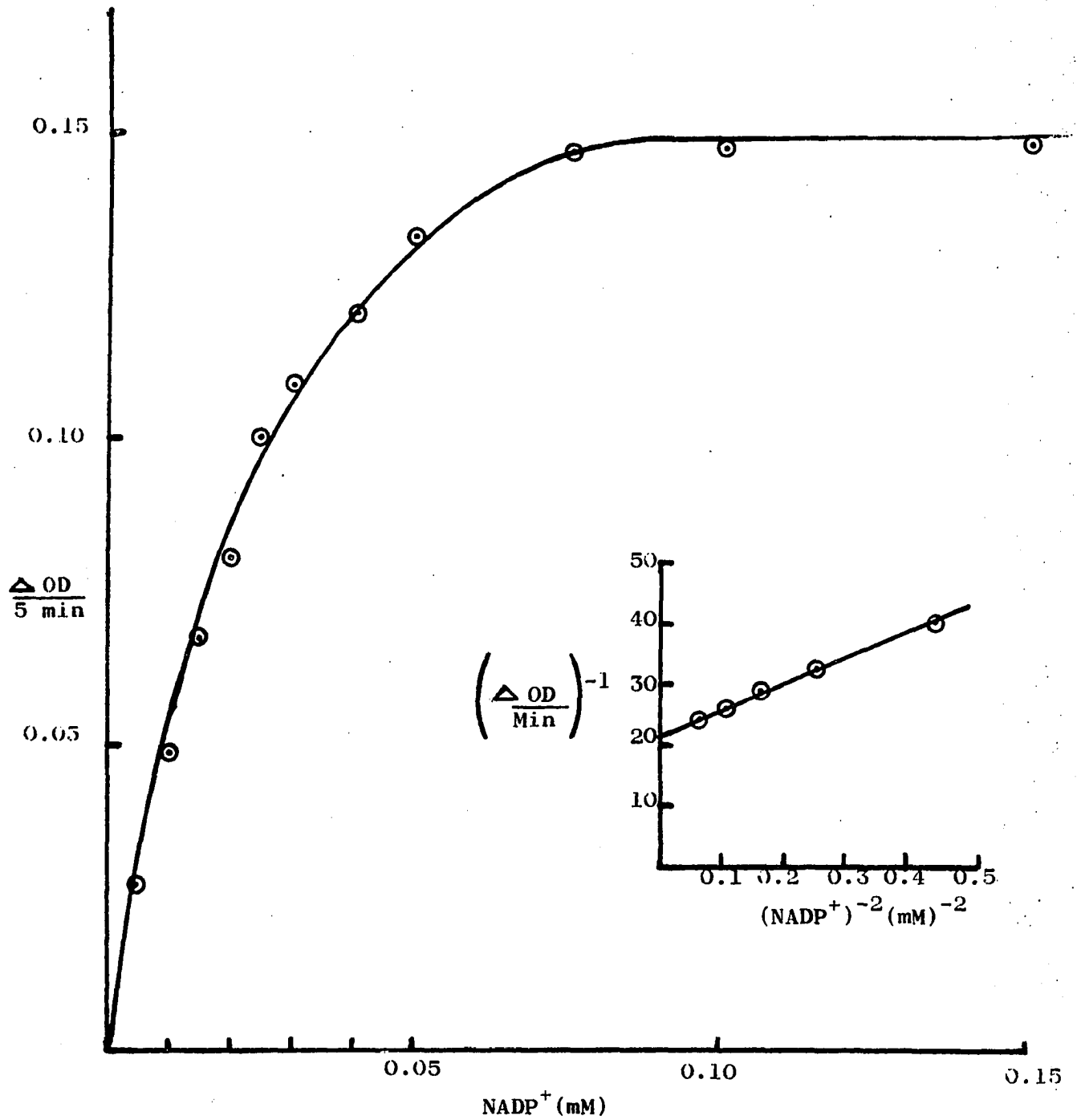


Figure 10:  $NADP^+$  saturation of GPDH from WI-38 VA13A. Abbreviations in Chapter III. Inset is the Lineweaver-Burk Plot corresponding to the saturation curve.

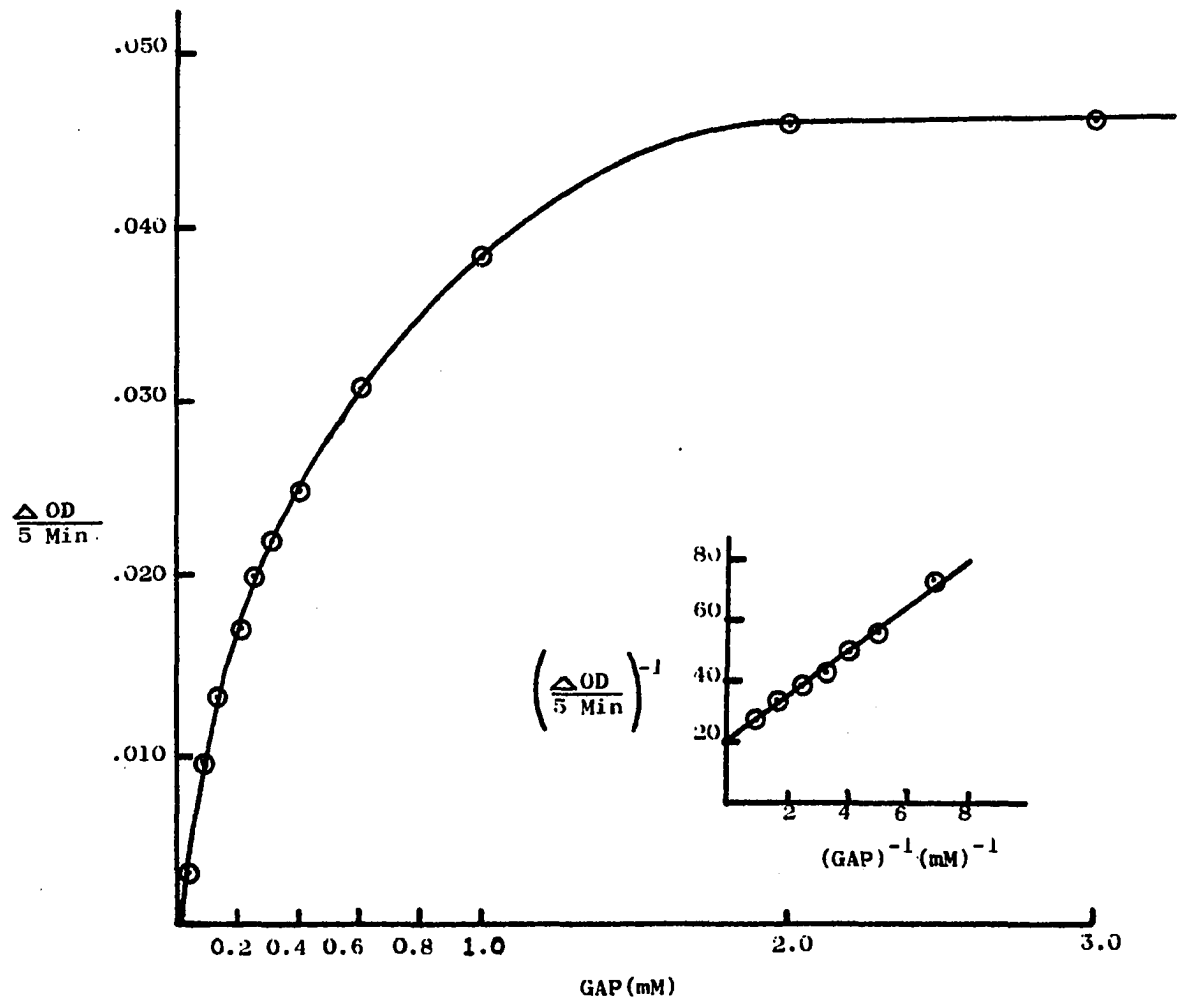


Figure 11: GAP saturation of GAPDH from WI-38. Abbreviations in Chapter III. Inset is the Lineweaver-Burk Plot corresponding to the saturation curve.

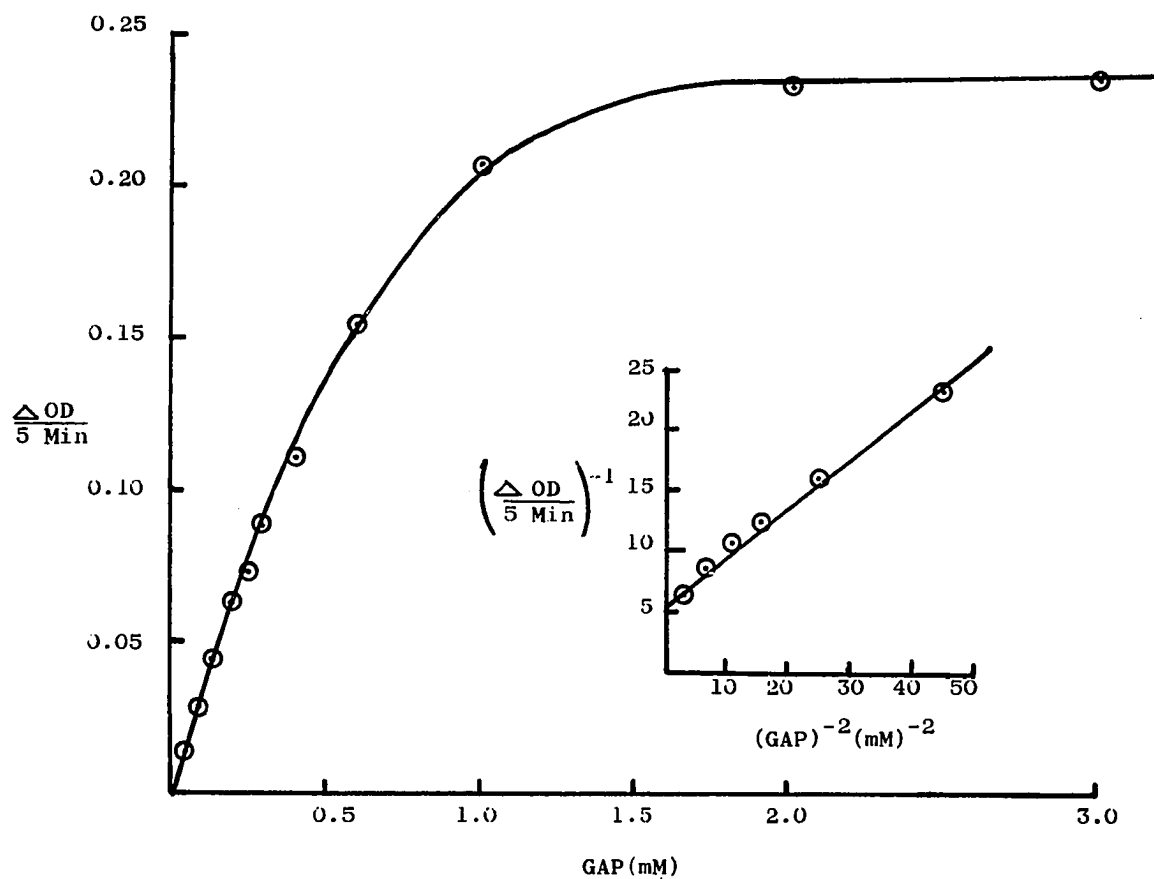


Figure 12: GAP saturation of GAPDH from WI-38 VA13A. Abbreviations in Chapter III. Inset is the Lineweaver-Burk Plot corresponding to the saturation curve.

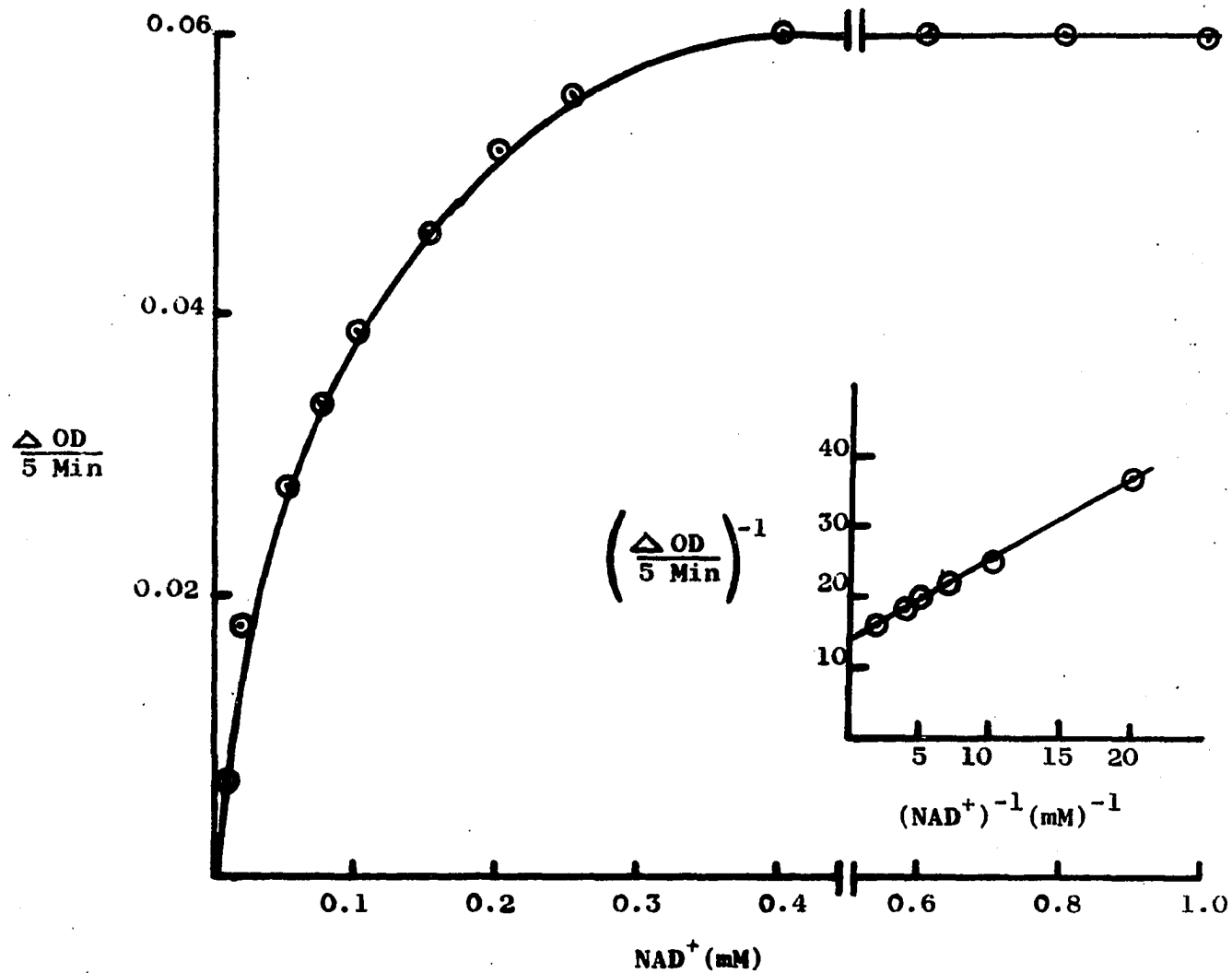


Figure 13:  $NAD^+$  saturation of GAPDH from WI-38. Abbreviations found in Chapter III. Inset is the Lineweaver-Burk Plot, corresponding to the saturation curve.

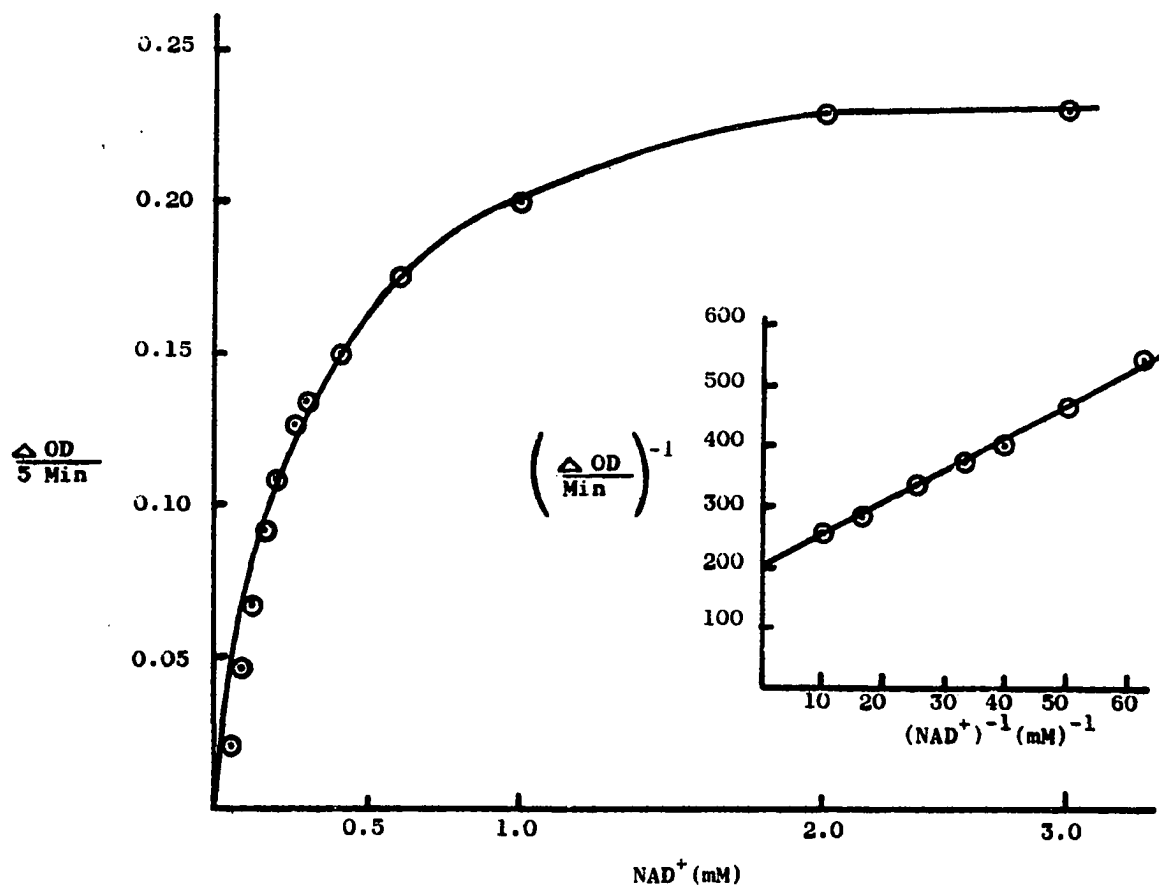


Figure 14:  $\text{NAD}^+$  saturation of GAPDH from WI-38 VA13A and corresponding Lineweaver-Burk Plot (inset). Abbreviations found in Chapter III.

54  
~~55~~

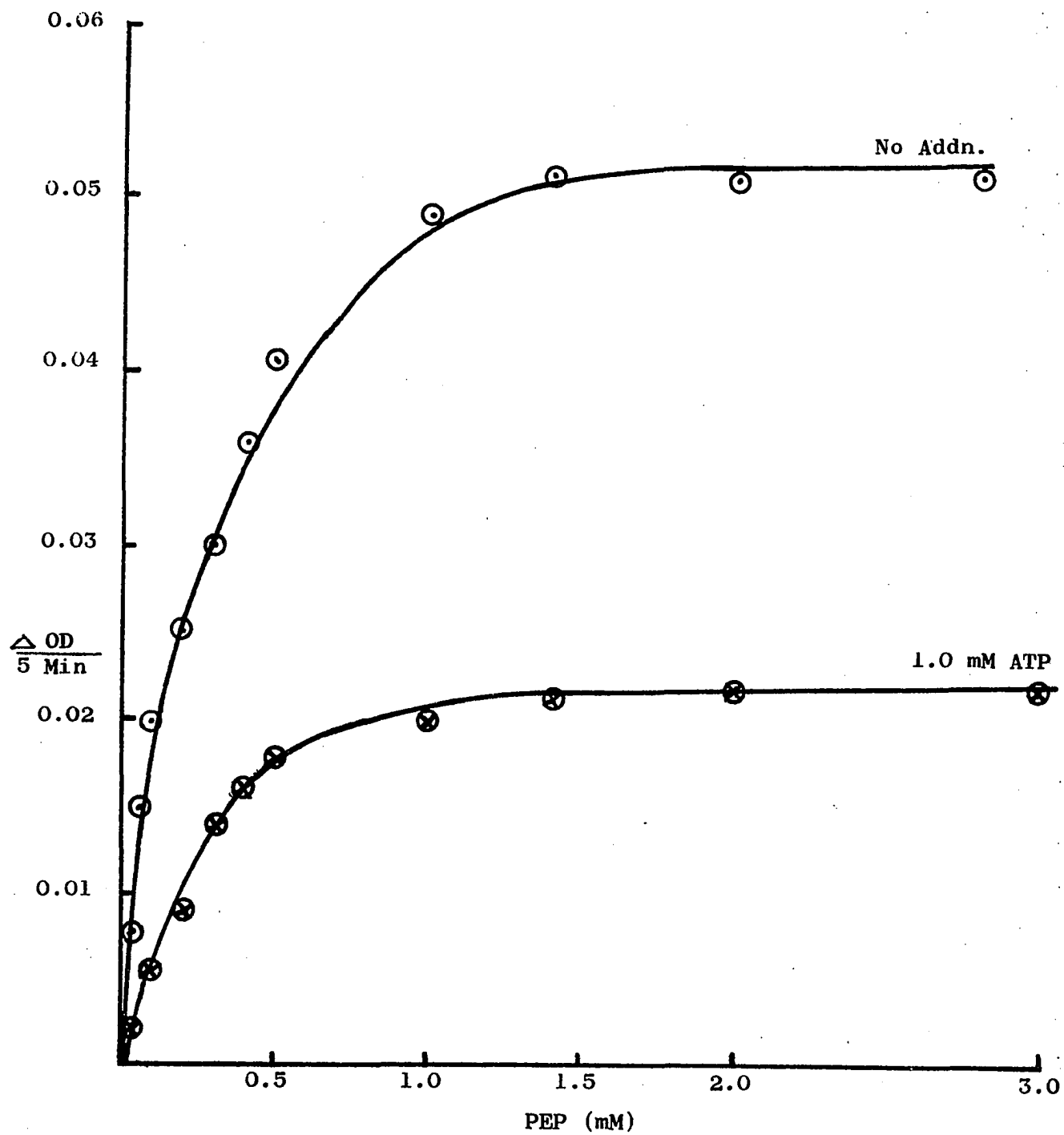


Figure 15: Effect of ATP on PEP saturation of PK from WI-38. Abbreviations in Chapter III.

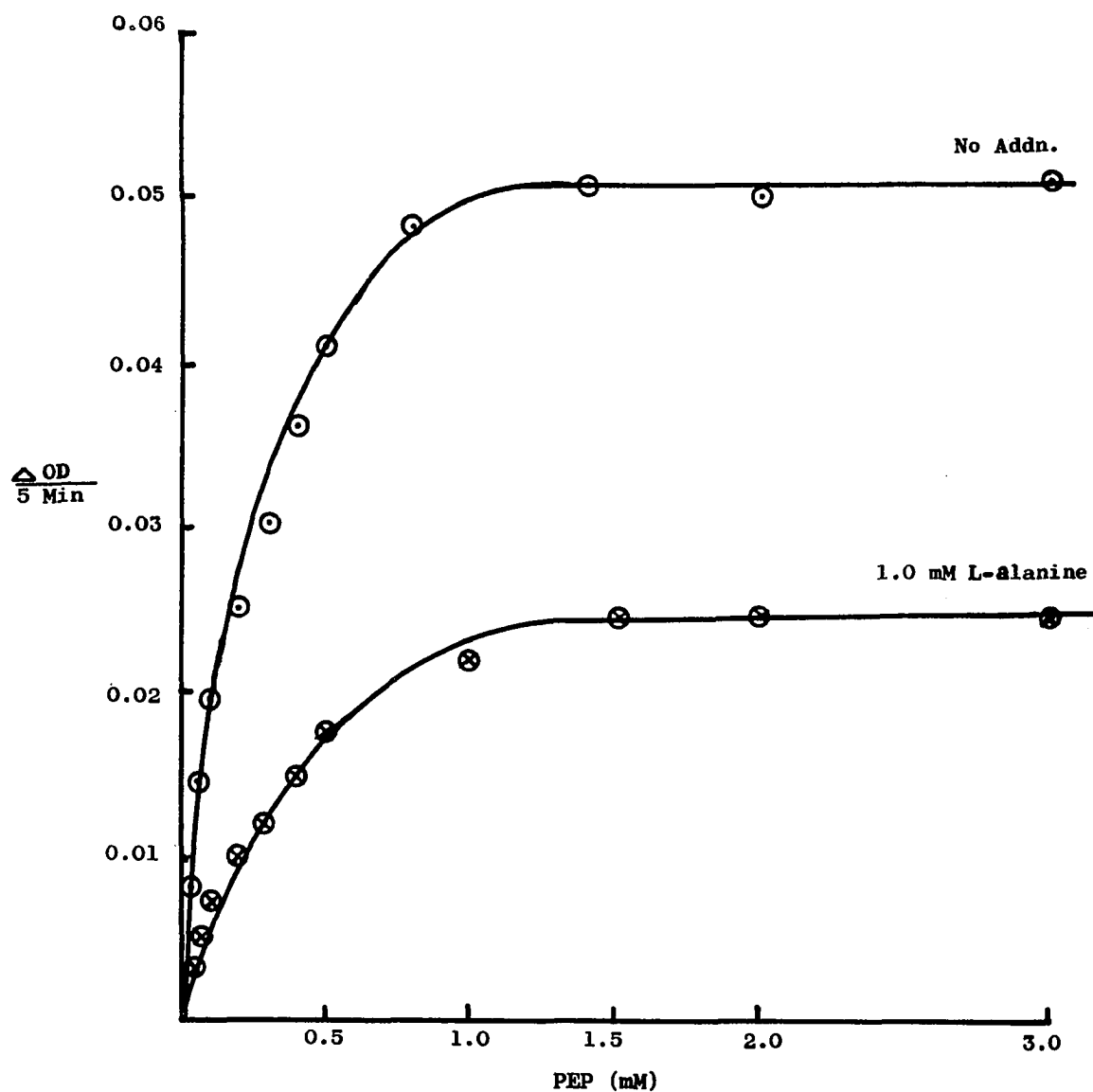


Figure 16: Effect of L-alanine on PEP saturation of PK from WI-38. Abbreviations found in Chapter III.



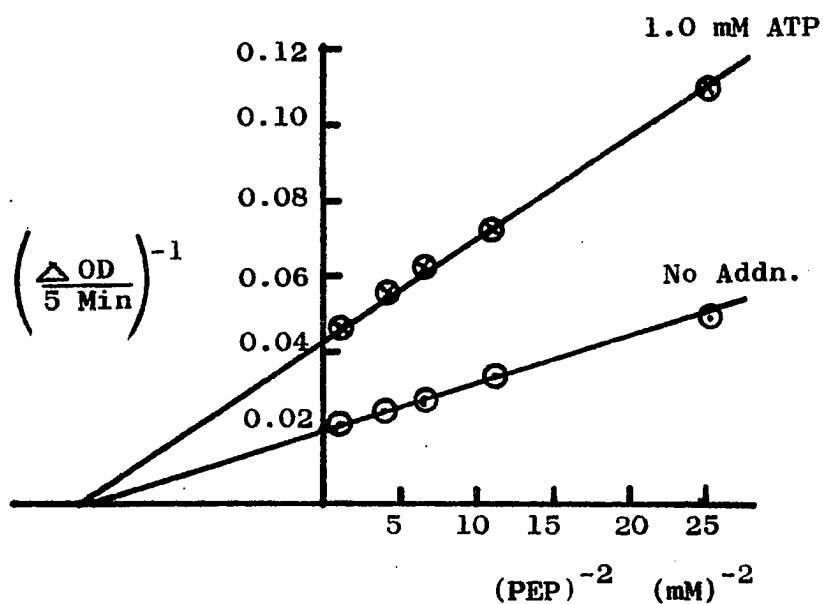
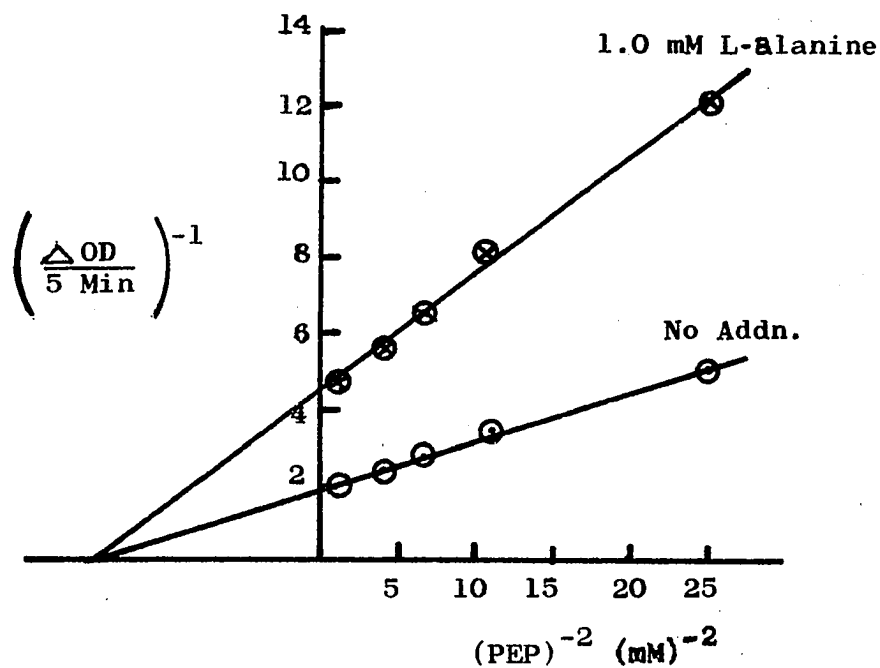


Figure 17: Effect of L-alanine (top curve) and ATP (lower curve) on Lineweaver-Burk Plot for PEP saturation of PK from WI-38. Abbreviations found in Chapter III.

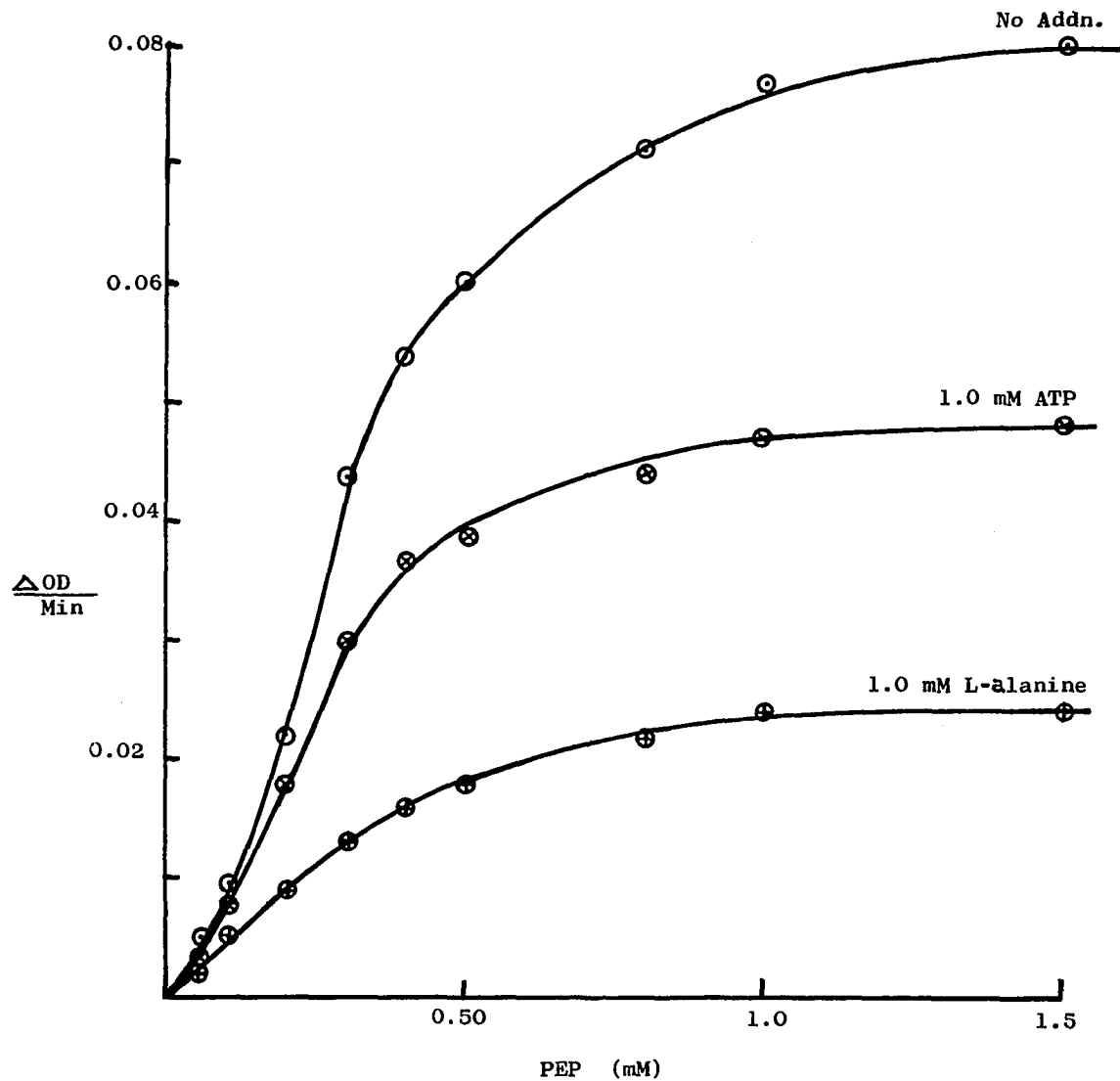


Figure 18: Effect of L-alanine and ATP on PEP saturation of PK from WI-38 VA13A. Abbreviations found in Chapter III.

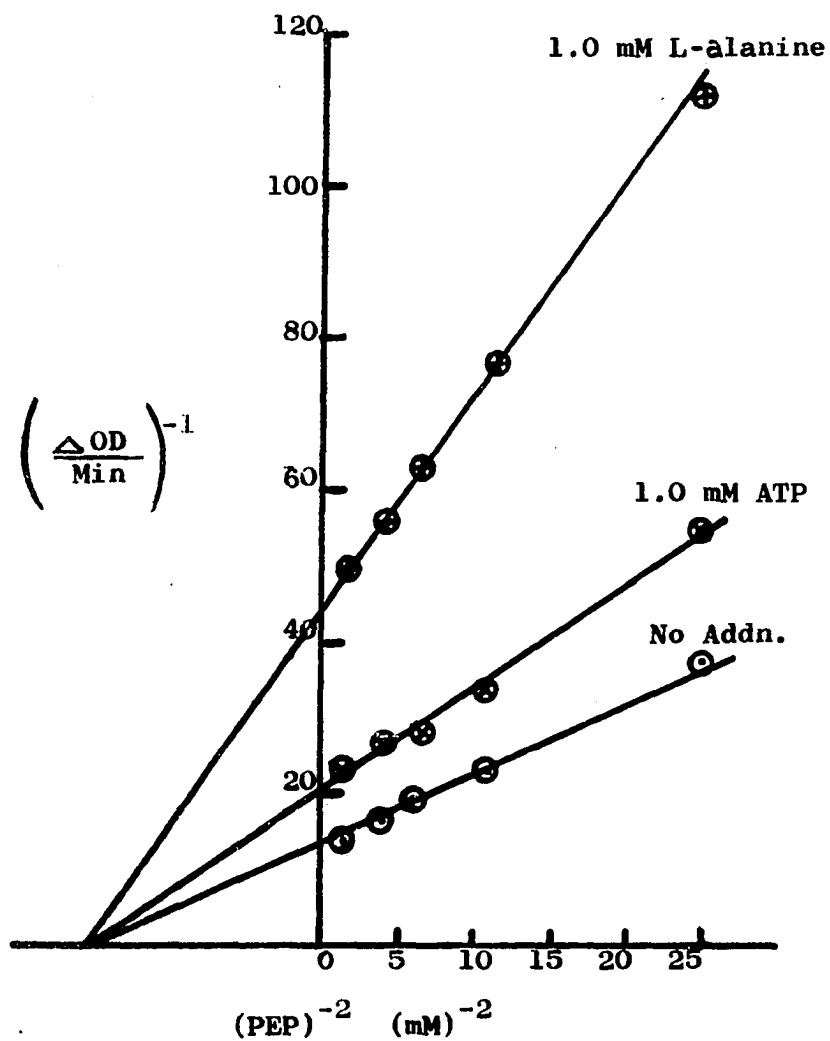


Figure 19: Effect of L-alanine and ATP on Lineweaver-Burk Plot for PEP saturation of PK from WI-38 VA13A. Abbreviations found in Chapter III.

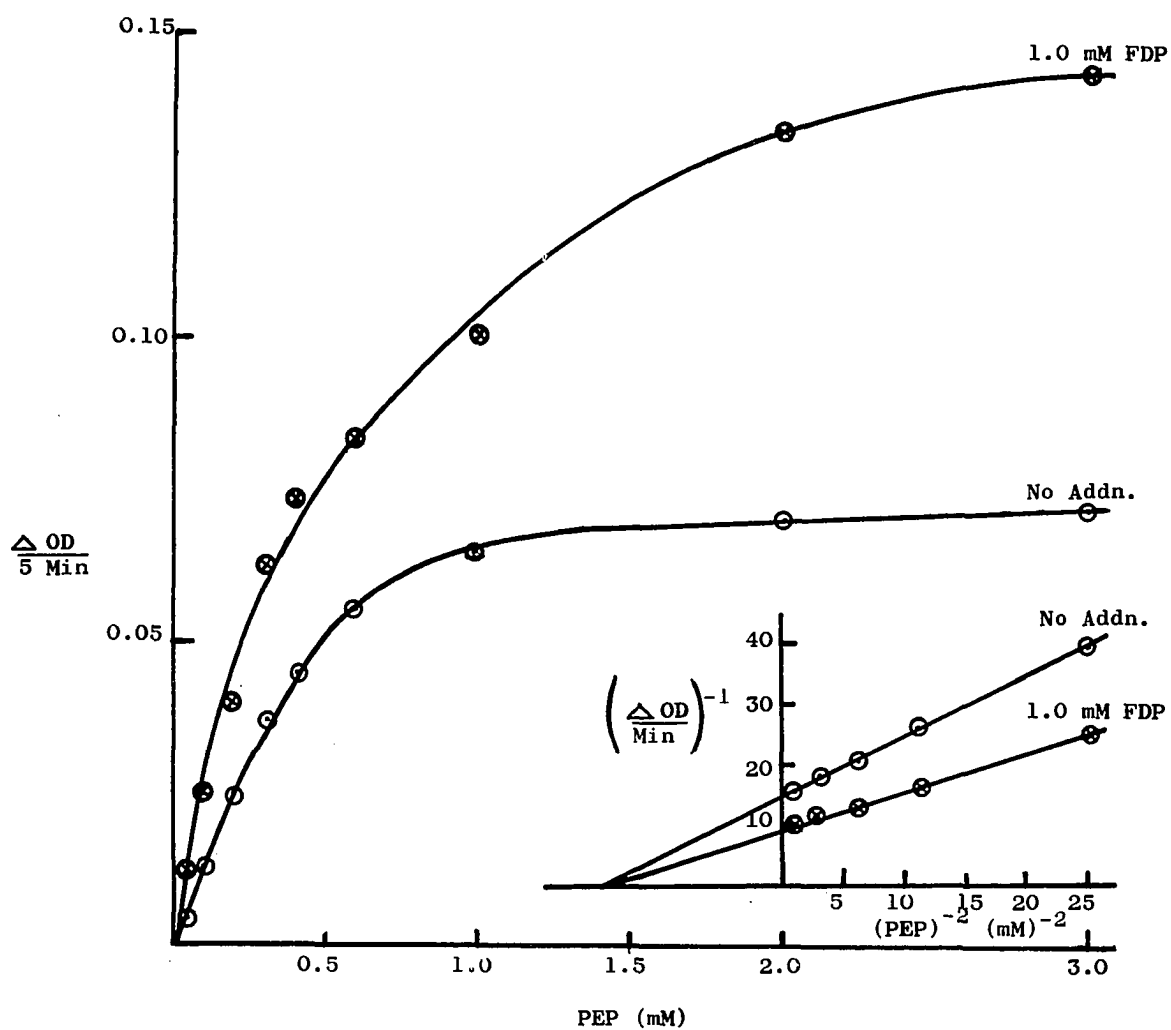


Figure 20: Effect of FDP on PEP saturation of PK from WI-38 VA13A. Abbreviations found in Chapter III. Inset is the Lineweaver-Burk Plots corresponding to the saturation curve.

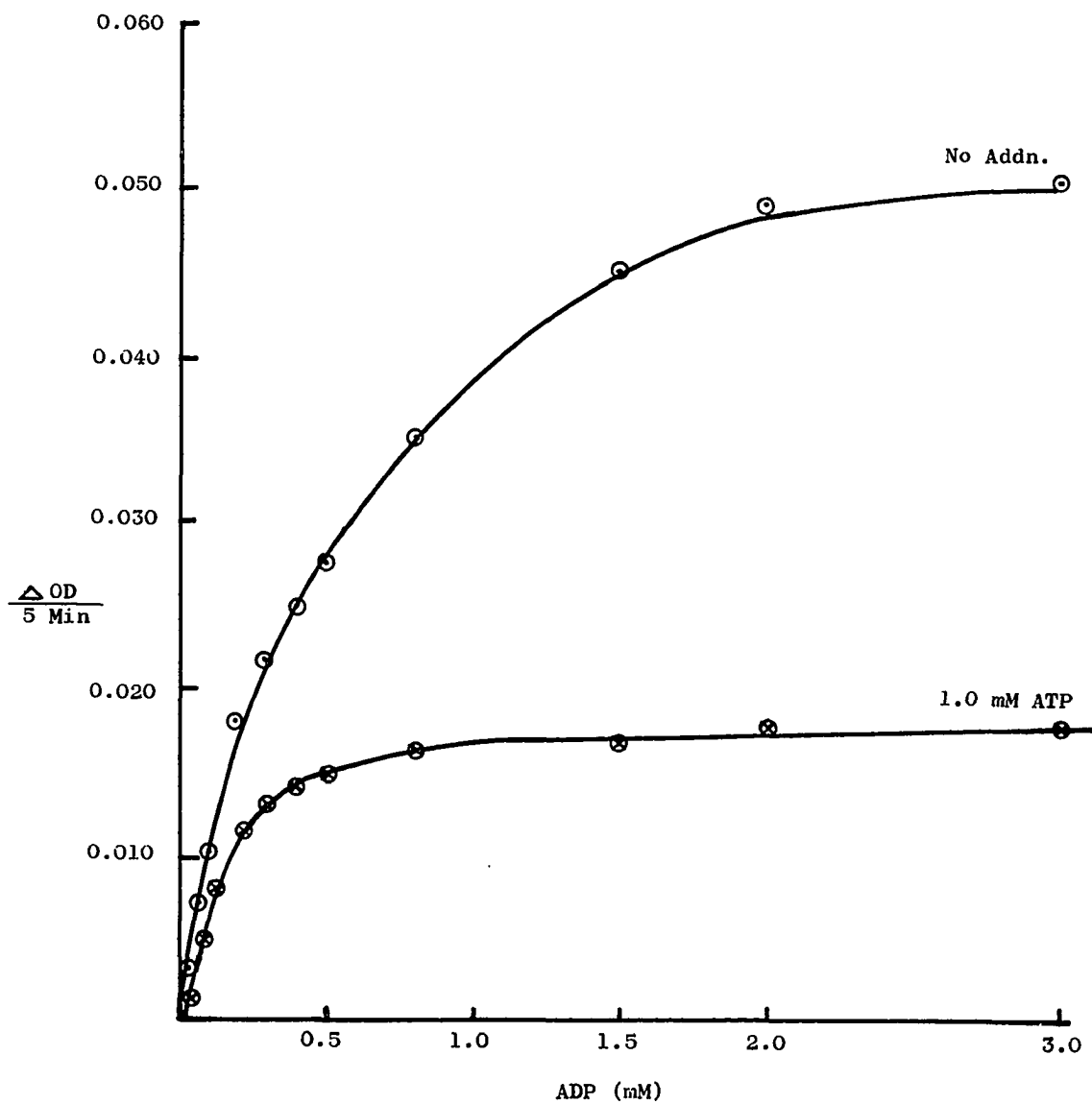


Figure 21: Effect of ATP on ADP saturation of PK from WI-38. Abbreviation found in Chapter III.

61  
~~62~~

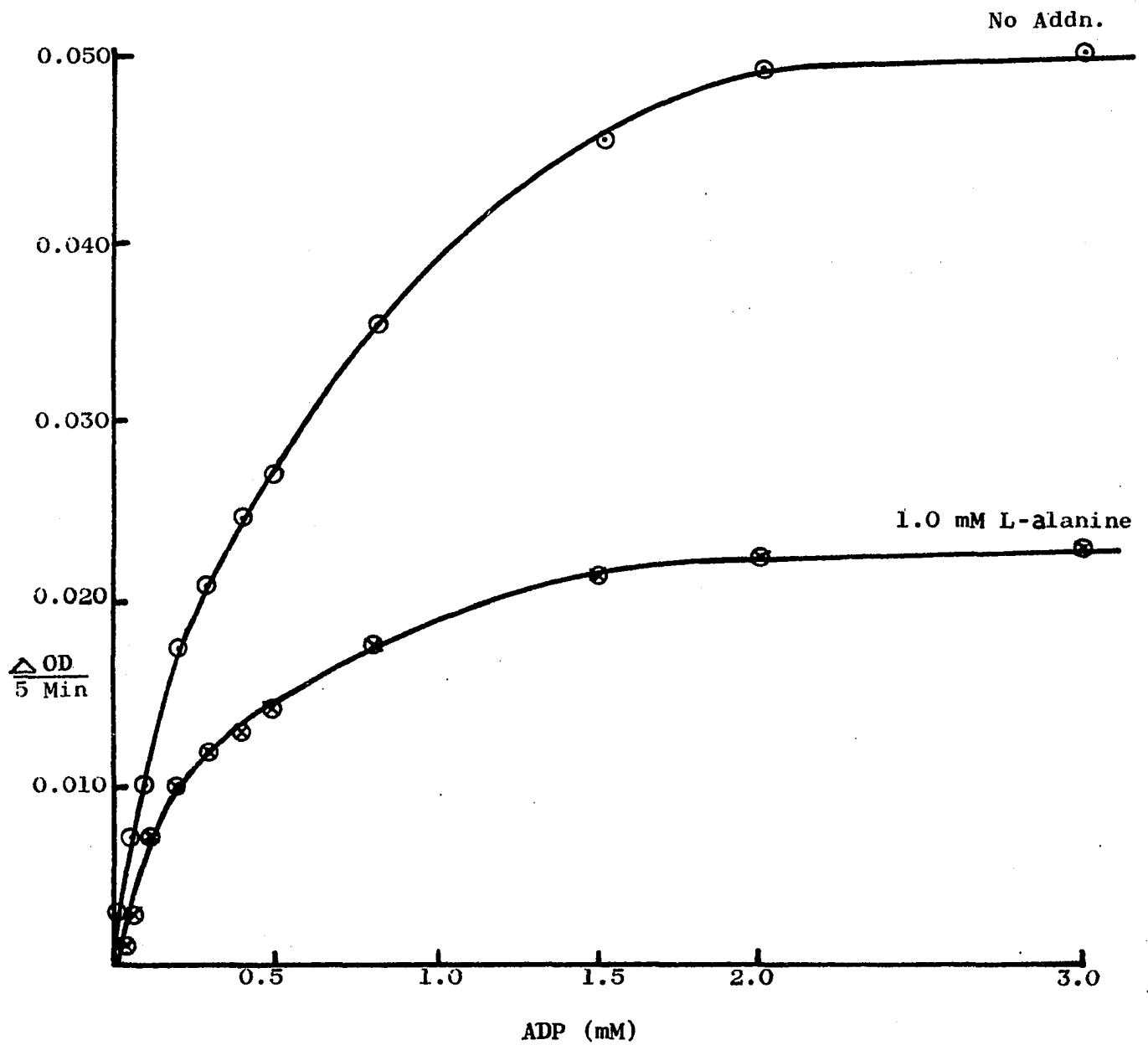
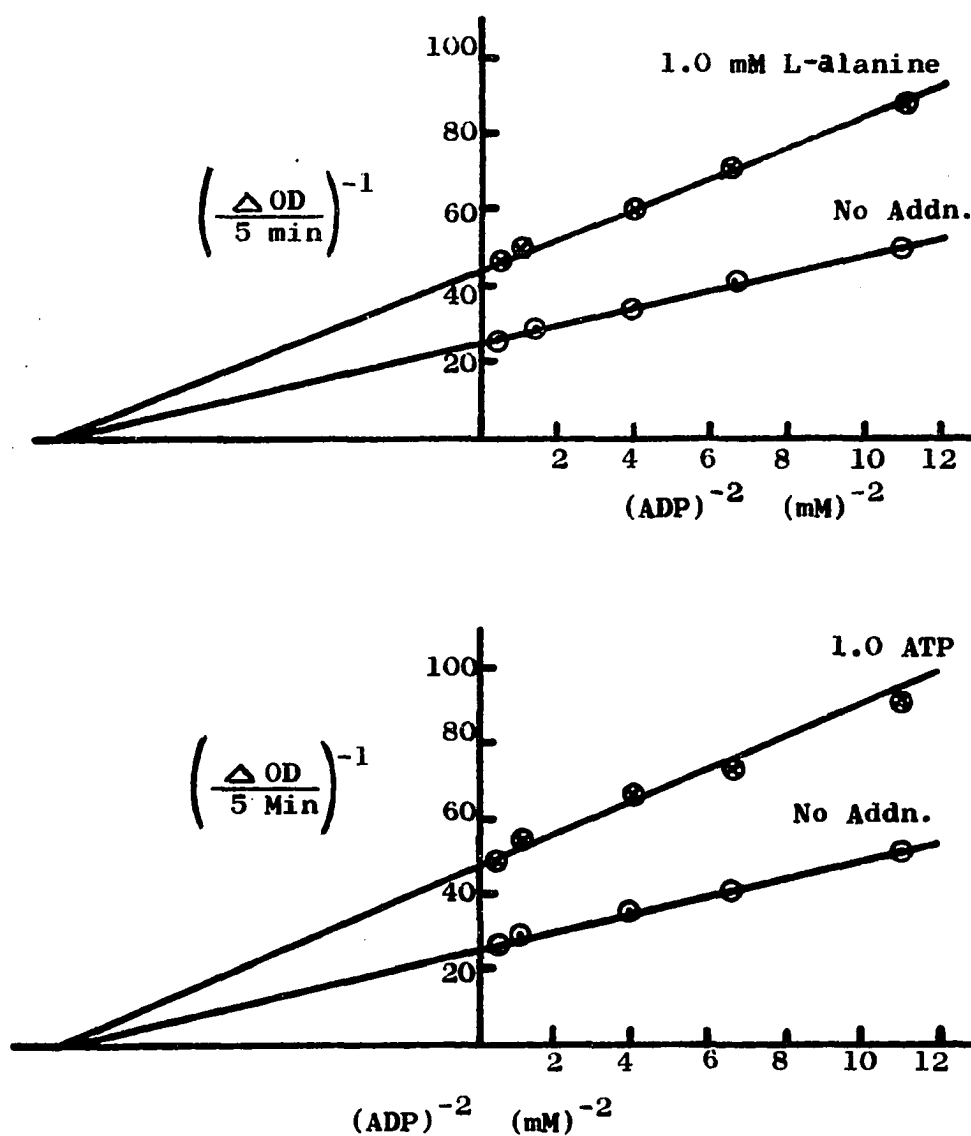


Figure 22: Effect of L-alanine on ADP saturation of PK from WI-38. Abbreviations found in Chapter III.



**Figure 23: Effect of L-alanine (top curve) and ATP (lower curve) on Lineweaver-Burk Plot for ADP saturation of PK from WI-38. Abbreviations found in Chapter III.**

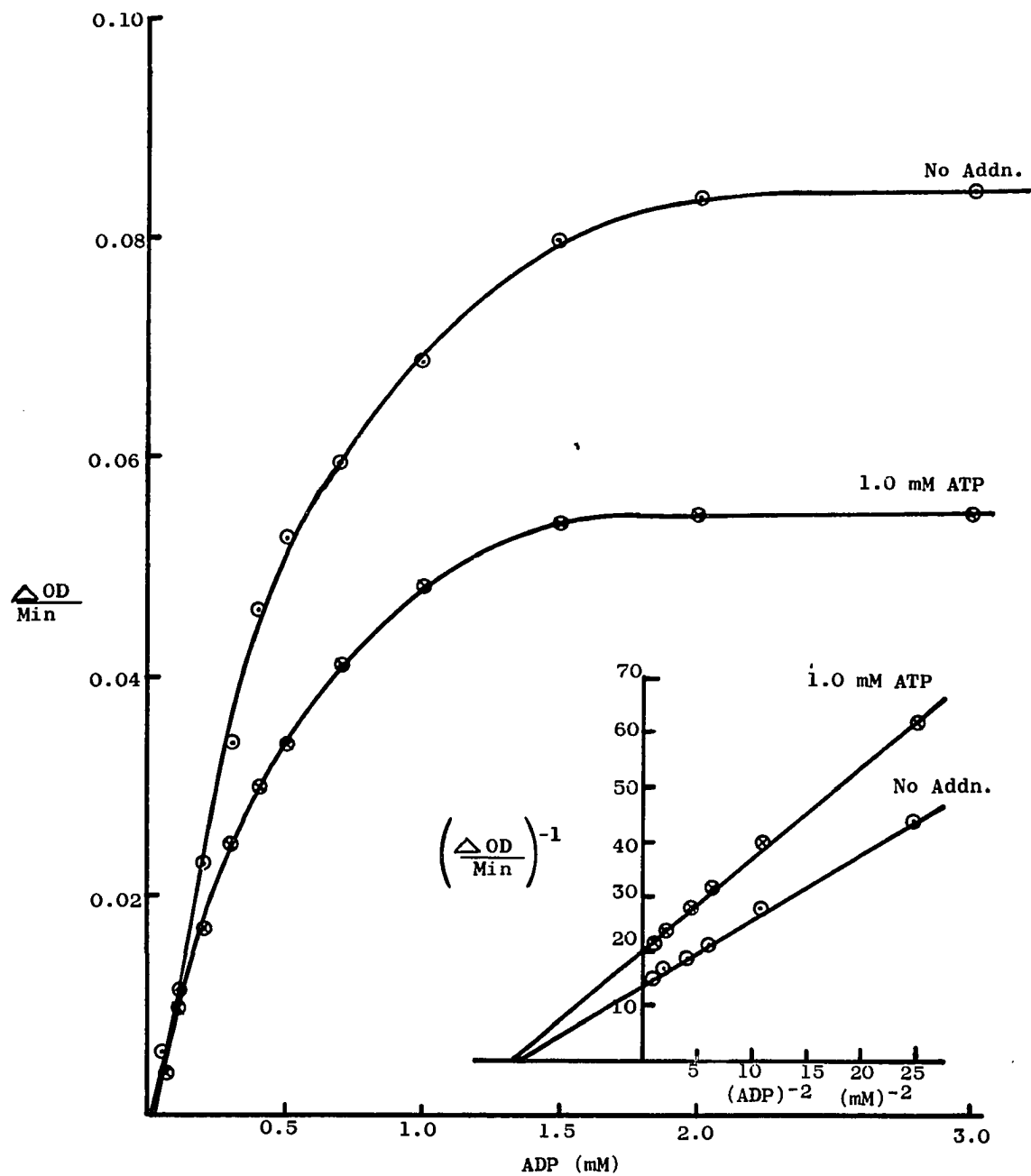


Figure 24: Effect of ATP on ADP saturation of PK from WI-38 VA13A. Abbreviations found in Chapter III. Inset is the Lineweaver-Burk Plots corresponding to the saturation curves.



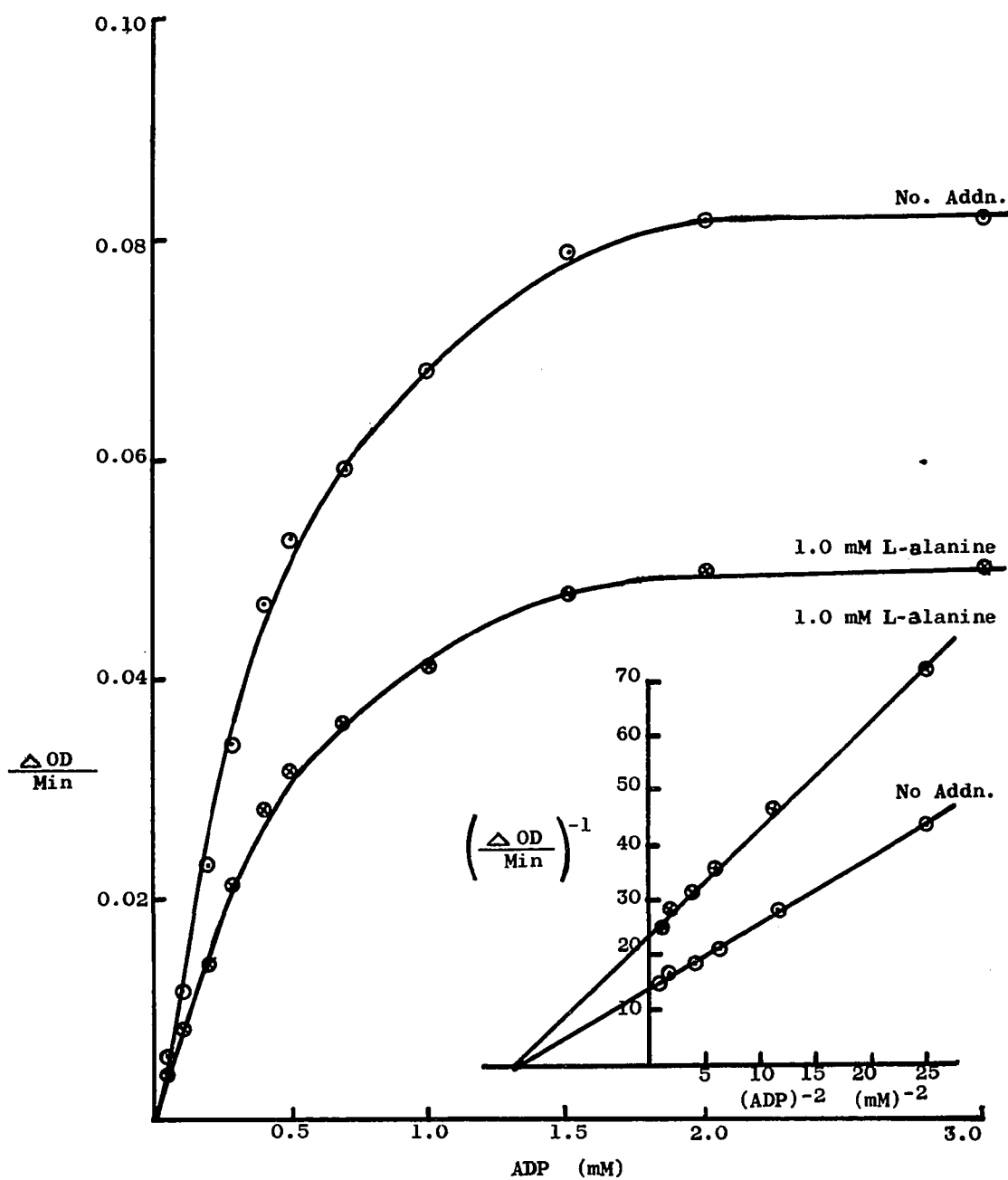


Figure 25: Effect of L-alanine on ADP saturation of PK from WI-38 VA13A. Abbreviations found in Chapter III. Inset is the Lineweaver-Burk Plots corresponding to the saturation curves.

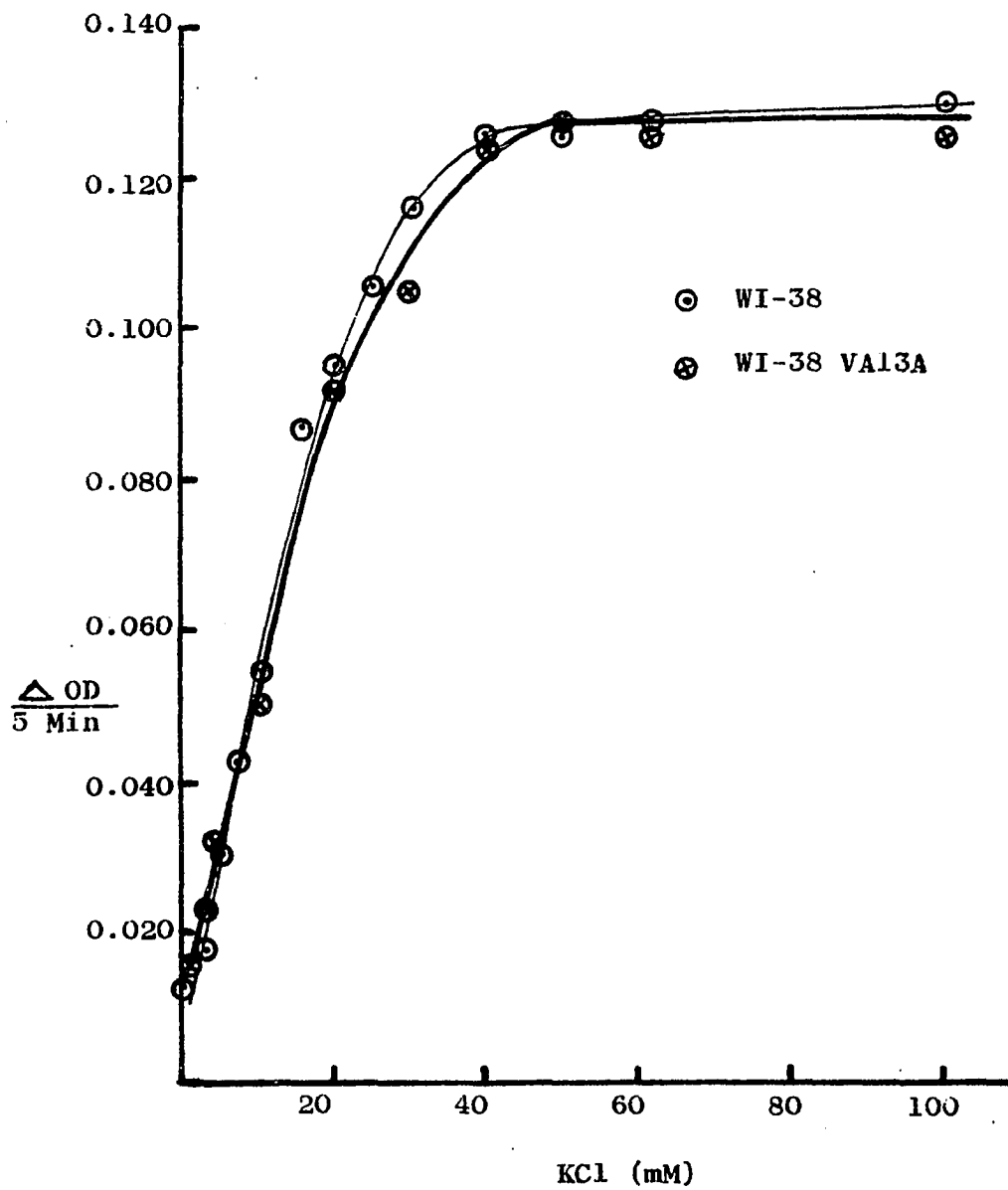


Figure 26: Activation of PK from WI-38 and WI-38 VA13A by KCl. Abbreviations found in Chapter III.

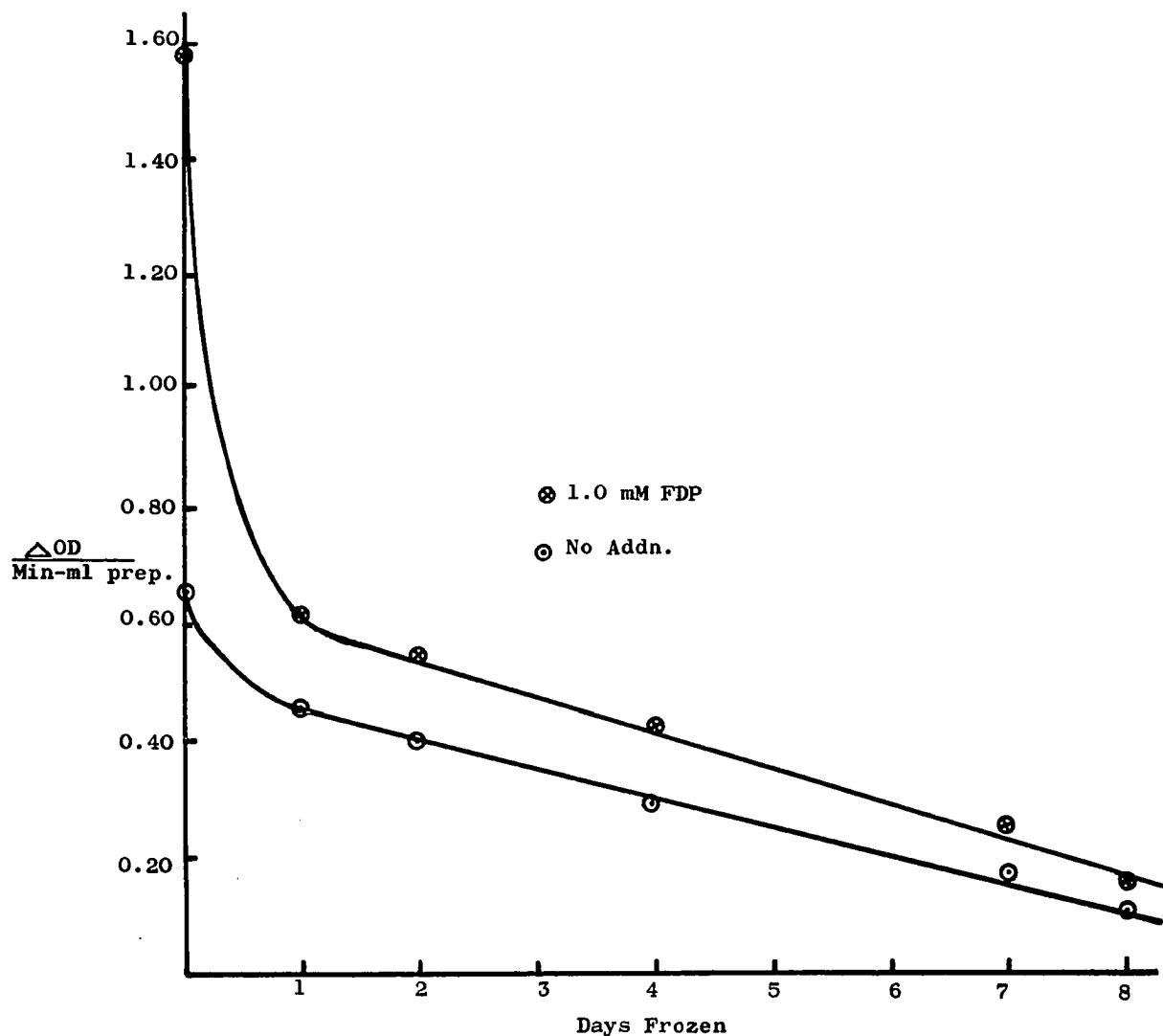


Figure 27: Desensitization of PK from WI-38 VA13A to FDP activation by storage at -20°C. Abbreviations found in Chapter III.

than 0.08 mM had to be squared in order to generate a straight line from the Lineweaver-Burk equation,  $\frac{1}{v} = \frac{K_m}{V_m} \frac{1}{[S]} + \frac{1}{V_m}$ . The reason for this operation as well as its implications will be explained in the discussion. Also for GPDH from both sources reciprocals of the concentration of  $\text{NADP}^+$  had to be squared in order to obtain a straight line from the Lineweaver-Burk equation. Also, for PK from both sources the reciprocal values of the concentrations of both substrates had to be squared in order to generate a straight line from the Lineweaver-Burk equation. The assays for each enzyme were made as outlined in Chapter III except that one substrate is varied over the concentration range given on the abscissa of each saturation curve.

Table 6 is a tabulation of the kinetic constants that can be determined from Figures 1 through 25.

By comparing the Michaelis Constants ( $K_m$ ) tabulated in Table 6, it is evident that the  $K_m$ 's are nearly identical with a few exceptions. The  $K_m$  of  $\text{NAD}^+$  for GAPDH seems to be different for the two cell types. For WI-38 the  $K_m$  is 0.065 mM and 0.085 mM and for WI-38 VA13A the  $K_m$  is 0.250 mM and 0.256 mM as determined from the saturation curve and Lineweaver-Burk plot, respectively. For PK the range of  $K_m$ 's for ADP varies significantly in both cell types, and  $K_m$  is dependent on the method of estimation. However, the  $K_m$  for ADP is about the same for each cell type when determined by identical methods. Since the  $K_m$  determination

is less valid for the saturation curve, the  $K_m$  from the Lineweaver-Burk plot is probably the more valid  $K_m$ .

TABLE 6.--Kinetic Constants tabulated for Figures 1-25.  
Abbreviations may be found in Chapter III. Michaelis  
Constants are given in millimole concentration

Enzyme	Substrate	Source	Michaelis Constant from:	
			Saturation Curve	Lineweaver-Burk Plot
HK	Glucose	WI-38	0.013	0.012
HK	Glucose	WI-38 VA13A	0.012	0.014
HK	ATP	WI-38	0.012	0.011
HK	ATP	WI-38 VA13A	0.010	0.011
GPDH	G-6-P < 0.08mM	WI-38	0.009	0.012
GPDH	G-6-P > 0.08mM	WI-38	0.040	0.039
GPDH	G-6-P < 0.08mM	WI-38 VA13A	0.012	0.014
GPDH	G-6-P > 0.08mM	WI-38 VA13A	0.040	0.039
GPDH	NADP <sup>+</sup>	WI-38	0.016	0.015
GPOH	NADP <sup>+</sup>	WI-38 VA13A	0.012	0.014
GAPDH	GAP	WI-38	0.340	0.333
GAPDH	GAP	WI-38 VA13A	0.320	0.290
GAPDH	NAD <sup>+</sup>	WI-38	0.065	0.085
GAPDH	NAD <sup>+</sup>	WI-38 VA13A	0.250	0.256
PK	PEP	WI-38	0.260	0.259
PK	PEP	WI-38 VA13A	0.280	0.259
PK	ADP	WI-38	0.400	0.300
PK	ADP	WI-38 VA13A	0.389	0.300

Figure 26 shows the activation effect of potassium ions on PK from WI-38 and WI-38 VA13A. This activation is determined in both sources by using a cell extract that had been sonicated in 0.050M tris buffer at pH 7.6, centrifuged, and dialyzed ( $\frac{1}{1000}$ ) against tris buffer, (pH 7.6). The procedure for obtaining a cell free preparation is identical to the one used for the enzyme assays except that tris buffer is substituted for the extraction solution. The assay method used is outlined in Chapter III.

As is noted from Figure 26, the KCl saturation curves for WI-38 and WI-38 VA13A are nearly superimposable. For both sources it is evident that the enzyme saturating level of KCl is about 50 mM for both types of cells.

In Figure 27 are shown the desensitization studies performed on PK from WI-38 VA13A. The cell free preparation was obtained as described in Chapter III, and then the activity was measured immediately for day zero. The cell free preparation was divided into five aliquots, was frozen at  $-20^{\circ}\text{C}$ , and was assayed on the days shown on the abscissa. The cell free preparation which was assayed immediately showed a 2.64 fold stimulation at 1.0 mM FDP. This stimulation rapidly dropped upon storage at  $-20^{\circ}\text{C}$ . After storage for 24 hours the FDP induces only a 1.35 fold stimulation. During the following days the activity of PK in the frozen solutions decreased, but the degree of activation remained reasonably constant. For example, the activation by FDP

was 1.35, 1.36, 1.38, 1.39, and 1.48 fold after being frozen for 2, 4, 7, and 8 days, respectively.

Table 7 is a compilation of the results of a comprehensive study which was made to find any modifiers of enzymatic activity that occur in these cell types. These results indicate that with the exception of the substrates none of the listed compounds affected the activity of HK.

For PK, ATP and L-alanine proved to be inhibitory at enzyme saturating levels of PEP and ADP. With respect to PEP, the inhibition by ATP (1.0 mM) was 58% and 47% and by L-alanine (1.0 mM) was 52% and 70% for WI-38 and WI-38-VA13A, respectively. With respect to ADP, the inhibition by ATP (1.0 mM) was 65% and 36% and by L-alanine (1.0 mM) was 55% and 41% for WI-38 and WI-38 VA13A, respectively. From Figures 17 and 19 it is evident that both ATP and L-alanine are non-competitive inhibitors with respect to PEP, and from Figures 23, 24, and 25 it is also evident that ATP and L-alanine are non-competitive inhibitors with respect to ADP regardless of the cell type. Also, KCl and FDP were shown to be activators of PK, 10 and 2 fold, respectively. As was discussed earlier PK from both cell types is strongly activated by KCl (see Figure 26), and as shown in Figure 20, FDP is a non-competitive activator of PK with respect to PEP.

For GAPDH only the adenine nucleotides (AMP, ADP, and ATP) affected enzymic activity. The degree of inhibition

TABLE 7.--Effect of selected compounds on the activity of HK, PK, GAPDH, and GPDH. Abbreviations and assay conditions may be found in Chapter III. All compounds were 1.0 mM in the assay

Compound	HK	PK	GAPDH	GPDH
Glucose	Substrate	No Effect	No Effect	No Effect
G-6-P	No Effect	"	"	Substrate
R-5-P	"	"	"	No Effect
F-6-P	"	"	"	"
FDP	"	Activator	"	"
GAP	"	No Effect	Substrate	"
3-PGA	"	"	No Effect	"
2-PGA	"	"	"	"
PEP	"	Substrate	"	"
Pyruvate	---	---	---	"
Lactate	"	---	---	"
Citrate	"	No Effect	No Effect	"
Isocitrate	"	"	"	"
$\alpha$ Ketoglutarate	"	"	"	"
Succinate	"	"	"	"
Fumarate	"	"	"	"
Malate	"	"	"	"
Oxaloacetate	---	---	---	"
ATP	Substrate	Inhibitor	Inhibitor	"
ADP	No Effect	Substrate	"	"
AMP	"	No Effect	"	"
3' -5' Cyclic AMP	"	"	No Effect	"
Inorganic Phosphate	"	"	Substrate	Inhibitor
L-alanine	"	Inhibitor	No Effect	No Effect
KCl	"	Activator	"	"



was not dependent on the degree of phosphorylation of the adenine nucleotide. At half saturating levels of GAP or  $\text{NAD}^+$  the adenine nucleotides (1.0 mM) inhibited GAPDH by 25 to 30%, and at enzyme saturating levels of both substrates these adenine nucleotides (1.0 mM) inhibited GAPDH by 10 to 12%.

Also from Table 7 it can be observed that GAPDH except for G-6-P was affected only by inorganic phosphate (1.0 mM) which inhibits about 30% at substrate saturating levels of the enzyme.

The effect of pyruvate on HK, PK, and GAPDH, the effect of lactate of PK and GAPDH and the effect of oxaloacetate (OAA) on HK, PK, and GAPDH were not reported because the presence of these compounds in the assay solution complicated the measurement of enzyme activity. Pyruvate and lactate complicate the PK and GAPDH assays by utilizing any  $\text{NADH}$  or  $\text{NAD}^+$ , respectively, since high LDH activity is present in the assay. Why pyruvate complicates the HK assay is unclear. However, the appreciable disappearance of absorption at 340 m $\mu$  that was observed in the HK blank could be due to endogenous  $\text{NADH}$  or conversion of any  $\text{NADPH}$  to  $\text{NADH}$  by the cell-free preparation. The  $\text{NADH}$  could then be used by any LDH in the assay. Since LDH activity could not be demonstrated in the presence of pyruvate and  $\text{NADPH}$ , a  $\text{NADPH}$  specific LDH is not complicating the assay. The effect of OAA on the PK and GAPDH activity was due to

the ability of LDH to use OAA as a substrate. The effect of OAA on the HK reaction is also unclear. However, it is thought that the effect is not an inhibition of HK, but a utilization of the NADPH produced by the coupling enzyme. Probably the OAA or some conversion product is utilizing the NADPH by a NADPH specific dehydrogenase, e.g. NADPH specific malate dehydrogenase.

## CHAPTER V

### DISCUSSION

Since the molar ratio of lactate production to glucose consumption is nearly 2 for each source, it is reasonable to assume that the ultimate fate of glucose is predominately lactate formation. These results agree with the general concept that cultured cells exhibit a relatively high aerobic glycolysis rate and a relatively low respiratory rate (39).

Kruse and Miedema (37) have reported a glucose uptake of  $0.324 \pm 0.077$  micromicromoles/hr/cell and a lactate production of  $0.334 \pm 0.099$  micromicromoles/hr/cell for WI-38 cultured under perfusion conditions. In a personal communication (36) Kruse has related a glucose uptake of  $0.233 \pm 0.099$  micromicromoles/hr/cell and a lactate production of  $0.355 \pm 0.099$  micromicromoles/hr/cell for WI-38 VA13A cells that were cultured under perfusion conditions. Kruse and Miedema do not demonstrate a statistically significant difference between the two cell types, but considering only the average, WI-38 shows a higher lactate production and glucose utilization. However, the data presented in Table 1

show that the glycolysis rate of WI-38 is statistically greater than that of WI-38 VA13A. Also a comparison of the magnitude of the data in Table 1 with that of Kruse and co-workers (37) and Cristofalo and co-workers (16) indicates that the data in Table 1 are about 10 fold greater than their data. It should be emphasized that Kruse and Cristofalo cultivated their cells under perfusion conditions while we used stoppered bottle cultivation. Therefore, it is probable that the difference in the data is a consequence of the method of cell cultivation.

As was discussed in Chapter I, cells transformed by Rous sarcoma viruses (52) have the same glycolytic capacity as uninfected cells, but the transformed cells exhibit a greater growth potential than the untransformed cells. Also, polyoma transformed cells exhibit a two fold greater glucose consumption than the untransformed cells (9). It is evident from a comparison of the glycolysis data of this work with glycolysis data from other non-transformed - transformed cell pairs that the viral transformations which were discussed do not have the same effect on the glycolysis rate. Seemingly, the effect of viral transformation on glycolysis is dependent on the transforming virus and probably on the host cell. Considering the magnitude of differences between the glycolytic rates (10) of rat liver and rat hepatomas, it can be seen that the advanced hepatoma glycolytic rate is 15 times the host liver whereas the

sub-minimal and minimal hepatoma's glycolytic rate is 2 to 3 times that of the host liver. Thus, the magnitude of change in glycolysis rate due to viral transformation by polyoma and SV40 viruses is relatively small, and it is comparable to the magnitude of change for minimal hepatomas compared to host liver. However, the SV40 transformed cells do not conform to the concepts of Warburg that malignancy is associated with increased fermentation (56).

By taking the glucose consumption and HK levels for both cell types from Tables 1, 3-A, and 3-B, Table 8 can be constructed:

TABLE 8.--Comparison of the HK levels and glucose consumption for WI-38 and WI-38 VA13A. The HK levels are given in millimicromoles of glucose utilized per minute per  $10^6$  cells, and the glucose consumption is given in micromicromoles per cell change per hour

Cell Type	Hexokinase Levels	Glucose Consumed
WI-38	$13.0 \pm 1.7$	$1.89 \pm 0.21$
WI-38 VA13A	$5.5 \pm 0.6$	$0.78 \pm 0.08$
Ratio $\frac{\text{WI-38}}{\text{WI-38 VA13A}}$	2.36	2.42

A comparison of the ratios for HK levels and glucose consumptions demonstrates that the correlation is striking and tempts one to explain the difference in glucose consumption on the basis of the HK level differences. This speculation is further strengthened by the data in Tables 3-A and 3-B

which indicate that HK is a low activity enzyme and under the proper conditions could be the rate limiting glycolytic enzyme. Therefore, the rationale for the explanation of the observed differences in the glucose consumption for WI-38 and WI-38 VA13A is well founded on the basis of HK levels. Thus, an explanation based on a viral induced change in the cell membrane which results in retardation of glucose permeability is unnecessary. An increase in glycolysis due to increased HK levels has also been found for other cells. For example, in advanced rat hepatomas increased glycolytic rate can be correlated with an increased level of HK (44).

In order to understand better the metabolic state of both types of cells, the intracellular concentrations of the adenine nucleotides (ATP, ADP, and AMP) were determined. The results of this study are presented in Tables 2-A and 2-B. These results show that WI-38 has the larger total adenine nucleotide pool and that the distribution of the particular nucleotide types is significantly different in the two cell sources. The lower level of adenine nucleotides in the viral transformed cell may be due to cellular leakage, depressed biosynthesis of adenine nucleotides, or increased catabolism of adenine nucleotides. Of the three possibilities none is particularly favored. Since respiration is relatively low in both cell types (18), it is probable that the regeneration of ATP is very low. Thus, the differences observed in the ATP levels may be due to greater

consumption of ATP in WI-38. The greater ATP consumption in WI-38 could be due to one or more of the following reasons:

(1) An increased protein synthesis (Miedma and Kruse (43) report high initial levels of protein in WI-38); (2) increased nucleotide transphosphorylation; and (3) increased ATP requiring ion translocation mechanisms. Another possibility which is based on experimental evidence that may contribute to the lower levels of ATP in WI-38 is the 3 fold greater activity of alkaline phosphatase in WI-38 compared to WI-38 VA13A (18).

In accordance with the concept of adenylate regulation of glycolysis (2) the higher ADP and AMP levels coupled with the decreased ATP levels are postulated to contribute to the higher glycolytic rate in WI-38 synergistic with the increased level of HK and GAPDH. This postulated difference in glycolysis is based on inference from work in other tissues (13, 29), but actual work will have to be performed on WI-38 in order to show the existence of AMP and/or ADP activation and of ATP inhibition of PFK as well as AMP inhibition of FDPase.

Of the enzymes investigated only HK, FDPase, GAPDH, GPDH, and 6PGADH are statistically different in WI-38 and WI-38 VA13A. In general, HK, GAPDH, and GPDH are 2 fold greater in WI-38 while 6PGADH is about 1.5 fold greater in WI-38, and FDPase is about 3 fold greater in WI-38. Although the statistical difference in specific activity of

PGI from both cell types is questionable, the PGI activity appears to be greater in WI-38 VA13A. In a similar study on WI-38 and WI-38 VA13A cells cultured in a perfusion system Cristofalo (14) also reports a higher activity of PGI in WI-38 VA13A as well as a greater activity (2 fold) for 6PGADH and transaldolase. He does not report significant differences for other glycolytic enzymes. No plausible explanation can be offered at this time for the differences observed between the two laboratories except that the cells were cultured by different methods. A related study on polyoma transformation (46) has shown that for the transformed cells HK,  $\text{NADP}^+$  specific isocitrate dehydrogenase, and  $\text{NAD}^+$  specific malate dehydrogenase specific activities are 2-3 fold greater than the non-transformed cell. However, GPDH activity in the non-transformed cell is 1-2 fold greater than in the transformed cell. Also, they found no statistical differences between the two sources for 6PGADH and LDH. In another related study on Rous sarcoma viral transformation (58) no significant differences in the specific activities of FDPase, GPDH and 6PGADH when compared to the host tissue are observed. However, for the viral transformed cell the specific activities of PGM, LDH, and PGI were 4 fold greater than in the non-transformed cells. From these data it is evident that no consistent trend in enzyme patterns which have been altered by viral transformation, can be shown at this time. Perhaps, when more information on the



enzyme patterns of various viral transformed and non-transformed cells is known, more generalizations can be made.

Even though the results in Chapter IV indicate that the enzymes showing statistically significant difference in activity from WI-38 and WI-38 VA13A do not exhibit any difference in substrate affinities ( $K_m$ 's) or pH profiles (with the possible exception of GAPDH), synthesis of a kinetically more active enzyme in WI-38 is possible and cannot be ruled out as a possible explanation. However, recent work (6) using enzyme-electrophoresis and enzyme immunoelectrophoresis indicates that GPDH for both sources is identical but that LDH from the two sources had different electrophoretic patterns. Thus, at least for GPDH the increase in specific activity is probably due to increased biosynthesis and this conclusion may very likely be extended to the other enzymes (6PGADH, HK, GAPDH, and FDPase). To explain the variation in enzyme levels between the two kinds of cells two possibilities exist: (1) the enzyme level is depressed in the transformed cell or (2) the enzyme level in the non-transformed cell is able to change for some reason and the transformed cell does not change. For example, Kruse (43) has shown for WI-38 that the activities of LDH and GPDH increase 3 fold after the cell sheet becomes confluent when compared to pre-confluent cells. The corresponding studies on WI-38 VA13A were not performed, but if it could be shown that the corresponding WI-38 VA13A enzyme levels did not

change with confluency, a plausible explanation for the difference in enzyme levels might be formulated. Two possible explanations for the effect of confluency on enzyme levels could be that the nutritional state of the medium of confluent cells is more depleted and induces an increased enzyme biosynthesis (this could be eliminated by perfusion techniques) or that the actual contact of the cells allows for the increased enzyme biosynthesis. Thus, the enzyme levels in WI-38 VA13A might not be altered by the nutritional state since it has been shown that the transformed cell is less limited by the nutritional state of the media than WI-38 or possibly the different outer cell membrane of the SV40 transformed cell does not permit induction of the enzymes. Even though the available data do not favor repression of certain enzymes in WI-38 VA13A, enzymic repression cannot be ruled out as a possible answer to the cause in enzyme differences.

Since PGI activity is greater in WI-38 VA13A, one cannot imply that this enzyme activity is always greater in WI-38. However, the higher PGI activity in the transformed cell may be a fortuitous alteration if not an adaptation mechanism. The higher PGI and lower GPDH activities in WI-38 VA13A would suggest that a larger fraction of the available G-6-P will be glycolyzed in WI-38 VA13A than used in the hexose monophosphate shunt. Since less G-6-P is theoretically formed in WI-38 VA13A, the differences

observed for these two enzymes may be necessary to insure sufficient glycolysis; thus, providing their "survival edge" over any other virus transformed cells which do not have this alteration. Some theoretical calculations, which may approximate the "in vivo" conditions, can demonstrate this hypothesis more vividly. By adding the activities of PGM, PGI, and GPDH and dividing the total into the activity of PGI, the fraction of G-6-P converted to F-6-P can be estimated. The fraction of G-6-P converted to F-6-P is 0.79 for WI-38 and 0.91 for WI-38 VA13A. This suspected lesser utilization of the hexose monophosphate shunt probably results in a reduced production of its products. This could result in less ribonucleic acid production due to lack of the precursor ribose-5-phosphate and could retard any metabolism which uses reduced triphosphopyridine nucleotide.

From Table 3-A and 3-B, it can be seen that aldolase controls triose phosphate formation and that GAPDH, even though of intermediate activity, appears to limit the rate of triose phosphate utilization for both cell classes. Consequently, the greater activity in WI-38 could give this cell a greater capacity for triose phosphate utilization than WI-38 VA13A and may then act synergistically with the increased HK, AMP, and ADP levels and decreased ATP levels to at least partly explain the increased glycolytic rate in WI-38.

In general, any difference in the specific activities of the statistically different enzymes is manifested as a 2 fold higher activity in WI-38. This 2 fold increase results in an approximately 2 fold increase in glycolysis. The cause of the relative increase in enzyme activity in WI-38 may be due to synchronous induction of these enzymes in WI-38 or synchronous repression in WI-38 VA13A. This behavior is similar to the results which led to the concept of functional genic units proposed by Weber, et al. (62).

It is interesting to compare the enzyme patterns of adult human lung (21) with the human embryonic lung tissue cultures, WI-38 and WI-38 VA13A (see Table 9).

TABLE 9.--Order of increasing glycolytic enzyme activity for WI-38, WI-38 VA13A, and human lung (21)

Order of Activity	Human Lung	WI-38	WI-38 VA13A
1	PFK	PFK	HK
2	Aldolase	Aldolase	PFK
3	HK	HK	Aldolase
4	GAPDH	GAPDH	GAPDH
5	LDH	LDH	PK
6	PGK	PGI	LDH
7	PK	PK	PGK
8	PGI	PGK	PGI

The lines in Table 9 divide the listed enzymes into three groups based on activity. These are arbitrarily designated high, intermediate, and low activity groups. The first three enzymes (HK, PFK, and Aldolase) fall into the low activity group while GAPDH falls into the intermediate group and is about 6 times as active as the low activity group enzymes. The last four enzymes which are about 4 to 5 fold greater than GAPDH are the high activity enzymes. From the comparison made in Table 9, it can be concluded that the enzyme levels within each activity group can change, e.g. as a result of viral transformation or of differentiation but that the enzymes generally found in each activity group do not change their group as a result of adaptation to tissue culture, viral transformation or differentiation.

Even though most of this discussion has been strongly slanted towards glycolysis, some comments on the effect of SV40 transformation of WI-38 on gluconeogenesis can be made. By comparing Tables 3-A and 3-B it is apparent that the FDPase activity in WI-38 is 3 times greater than the WI-38 VA13A enzyme. This 3 fold increase could lead to a greater rate of storage of glycogen in WI-38, but comparison of the glycogen levels in WI-38 and WI-38 VA13A would have to be made as well as a comparison of the gluconeogenic enzymes, pyruvate carboxylase and PEP carboxykinase, to prove this speculation.

As was related in Chapter IV, the statistically different glycolytic enzymes (HK and GAPDH) as well as GPDH and PK were studied. This was done by determining their pH profiles and kinetic constants.

Hexokinase has a pH profile that is nearly superimposable for both cell sources as well as identical optimum pHs (7.7). Another pH optimum at pH 9.0 was found, but this is the glucose dehydrogenase activity of the assay enzyme GPDH. By comparing the  $K_m$ 's in Table 6 for both cell types, it is evident that the HK from both cells is kinetically identical. By examining Table 4, it is indicated that the interaction coefficients for both substrates are nearly one, and thus, no interacting binding sites are found for HK. Table 7, indicates that of the compounds tested only the substrates affected the activity of HK. The lack of any affect by G-6-P on HK was surprising since G-6-P inhibition of HK has been found in a variety of sources (rat heart (21), rat brain (32), human erythrocytes (49), and ascites tumor cells (55)). Comparison of the  $K_m$ 's for ATP and glucose with the above sources indicates that the HK in the human embryonic lung is much more sensitive to its substrates. For example, the glucose  $K_m$  for rat tissue was  $0.045$  mM which is 3 fold greater than the human embryonic lung tissue, and the  $K_m$  for ATP is about  $0.5$  mM in ascites cells as well as rat cells which is forty fold greater.

GAPDH from WI-38 and WI-38 VA13A has pH profiles that approximately overlap and that exhibit the same pH optimum (pH 7.8). A physically similar type of curve has been reported for GAPDH from rabbit muscle, heart, and liver (7), but the pH optimum is much higher in rabbit tissues (pH 8.5-8.8). Comparison of the interaction coefficients in Table 4 indicates that the GAP coefficients are identical for both sources (1.5), and comparison of the  $\text{NAD}^+$  coefficients indicates a small but definite difference is found for WI-38 (1.0 to 1.2) compared to WI-38 VA13A (1.4 to 1.5). From Table 6 it can be observed that the  $K_m$  for GAP is very close for both sources (0.29 to 0.34 mM); however, the  $K_m$  for  $\text{NAD}^+$  is 3 to 4 fold less in WI-38 (0.065 to 0.085 mM) than in WI-38 VA13A (0.28 to 0.26 mM). From examination of the insets of Figures 11-14, it is evident that the reciprocal values of the GAP concentration have to be squared in order to obtain a straight line for WI-38 VA13A from GAPDH. By combining this information with the  $K_m$  and interaction coefficient data, it is evident that the affinity and binding site interactions are different between the WI-38 and WI-38 VA13A enzyme. This could be due to synthesis of a different enzyme by the viral transformed cell that has approximately the same affinity for GAP but has a greater interaction of GAP binding sites. This would explain why the reciprocal values of GAP concentration must be squared for the Lineweaver-Burk plot. Also, this viral induced

enzyme has a reduced affinity for  $\text{NAD}^+$  and possibly less interaction of the  $\text{NAD}^+$  binding sites. However, I feel that since the protein concentration in the WI-38 sonicate is less than in the WI-38 VA13A sonicate, more dissociation of the enzyme could occur in the WI-38 sonicate which may explain the difference in the kinetic parameters for both sources. Deal (19) has shown rabbit muscle GAPDH is dissociated faster by ATP at lower protein concentrations (0.1 mg/ml). If the degree of dissociation of GAPDH from WI-38 is the explanation of these results then the implication is that the  $\text{NAD}^+$  affinity of the dissociation products is greater than that of the whole enzyme and since the specific activity of GAPDH is greater in WI-38 (see Tables 3-A and 3-B) it is possible that the dissociation products are catalytically more active. Another factor that suggests enzymic dissociation is the necessity of squaring the reciprocal values of the concentration of GAP for the Lineweaver-Burk plot for WI-38 in order to produce a straight line. Thus, it seems that interaction of the GAP binding sites is reduced which is what might be expected as a result of enzymic dissociation.

In Table 7 it is shown that with the exception of the substrates only the adenine nucleotides (AMP, ADP, and ATP) affect the rate of GAPDH. The extent of this inhibition is dependent on the concentration of its substrates. At one-half saturating levels of GAP or  $\text{NAD}^+$ , the adenine



nucleotides (1.0 mM) inhibited GAPDH by 25 to 30%, and at enzyme saturation levels of both substrates these adenine nucleotides (1.0 mM) inhibit GAPDH by approximately 10%. At higher concentrations of substrates the inhibition is even further relieved indicating that the adenine nucleotides are not noncompetitive inhibitors. Inhibition of GAPDH by adenine nucleotides has been shown for rabbit muscle (19, 45), rabbit heart (45), and yeast (45, 51, 64). This type of inhibition has been characterized for several sources as mixed inhibition in rabbit tissues (45) and competitive in yeast (45, 51, 64). For rabbit tissues (46) the degree of phosphorylation does not affect the degree of inhibition by the adenine nucleotides; whereas, for yeast GAPDH (64) cyclic AMP is a very potent inhibitor (70% at 1 mM), while AMP, ADP, and ATP inhibit by 18, 14, and 10%, respectively. Deal and co-workers hypothesize that for yeast GAPDH the two nucleotide moieties of  $\text{NAD}^+$  have almost totally independent functions, the adenine nucleotide moiety is responsible for binding and the nicotinamide nucleotide moiety for catalysis. They found that a series of adenine containing compounds produced three distinct but related effects on yeast GAPDH activity and structure. They are (1) instantaneous inhibition of enzyme activity by AMP, ADP, ATP, and cyclic AMP due to competition with  $\text{NAD}^+$  for the  $\text{NAD}^+$  binding site on the enzyme (64); (2) a slow loss of enzymic activity produced by AMP, ADP, and ATP due to a slow, marked structural

change (51, 64); and (3) a very rapid loss of activity produced by ADP and ATP in the presence of chymotrypsin due to an induced structural change (64). Comparison of the GAPDH from human embryonic lung tissue with yeast and rabbit GAPDH indicates that even though each enzyme possesses individual characteristics, they have many common properties. For example, the initial affect of adenylates is the same for all three sources.

For GPDH from WI-38 and WI-38 VA13A, the pH profiles were identical with a pH optimum at 8.0. Examination of Table 4 indicates that at a concentration of G-6-P less than 0.08 mM, the interaction coefficients are nearly one for both cell types; and at a G-6-P concentration greater than 0.08 mM, the interaction coefficients are about two. The same type of change is also observed for  $\text{NADP}^+$  for both cell types. These results were found when it was observed that the Hill plots could be drawn with two slopes for G-6-P and  $\text{NADP}^+$  for WI-38 and WI-38 VA13A. The implication is that at a G-6-P concentration less than 0.08 mM and at a  $\text{NADP}^+$  concentration less than 0.10 mM very little, if any, interaction of the substrate binding sites occur, and at substrate concentrations greater than these, interaction of the substrate binding sites does occur, or that two GPDH isozymes exist one of which has interacting binding sites for G-6-P and  $\text{NADP}^+$ . From Table 6 it is evident that the affinity of GPDH is dependent on the concentration of G-6-P while the

affinity for  $\text{NADP}^+$  does not seem to be dependent on  $\text{NADP}^+$  concentration regardless of the kind of cell. Also, examination of Figures 5 and 7 indicates that the G-6-P saturation curves are not hyperbolic but possess an intermediate plateau. The corresponding Lineweaver-Burk plots (Figures 6 and 8) indicate that in order to obtain a straight line the reciprocal values for the concentrations of G-6-P may be plotted directly below 0.08 mM and must be squared above 0.08 mM. A composite picture of these results is that below a G-6-P concentration of 0.08 mM the concentration of substrate to give half maximum velocity  $(S)_{0.5}$  for G-6-P is about 0.01 mM, and the interaction coefficient is approximately one. Above a G-6-P concentration of 0.08 mM the  $(S)_{0.5}$  for G-6-P is 0.040 mM and the interaction coefficient is nearly 2.0. Before reaching a G-6-P concentration of 0.08 mM the GPDH activity appears to be very nearly saturated; however, at a G-6-P concentration of 0.08 mM the GPDH activity increases and finally becomes constant at 0.15 mM G-6-P. The binding of  $\text{NADP}^+$  seems to be analogous to the G-6-P binding. The  $\text{NADP}^+$  binding sites appear to interact but the affinity for  $\text{NADP}^+$  is not significantly changed. To explain these results, two possibilities exist: (1) two isozymes, one of which has interacting G-6-P binding sites, or (2) one enzyme that exhibits negative cooperativity. Examination of the dashed lines in Figures 5 and 7 show how the experimental data can be extended to

simulate two overlapping saturation curves. These data also fit the criteria of Koshland and co-workers for negative co-operativity (53), i.e. (1) the enzyme must possess a total of more than two substrate binding sites and (2) the relative magnitude of the intrinsic catalytic or binding constants of these sites first decreases, then increases as the enzyme is saturated which results in an intermediate plateau region in the enzyme saturation curve. From considering the initial velocity equation for a two-site model enzyme, they also concluded that, "neither a single enzyme with two substrate binding sites nor a mixture of enzymes, each with one substrate binding site, in the presence or absence of effectors, will yield curves possessing an intermediate plateau region, provided that both the rate of binding is rapid relative to the rate of catalysis (53)." Seemingly, a discrepancy exists between the GPDH data and Koshland's criteria, i.e. the Hill plots for GPDH indicate the occurrence of two interacting sites. But, by dialysis of the GPDH containing solution it was found that GPDH has significantly high endogenous activity for both substrates. The implication is that at least one G-6-P and  $\text{NADP}^+$  moiety are tightly bound to the enzyme. Thus, the Hill plots probably show only two weaker binding sites, and Koshland's criteria for the existence of more than two binding sites is satisfied. Luzzatto (41) has reported that the  $\text{NADP}^+$  saturation curve of GPDH from human erythrocytes is sigmoidal,

the interaction coefficient is about 1.7, and a transition from low ( $K_s = 0.045$  mM) to high ( $K_s = 0.013$  mM) affinity for  $\text{NADP}^+$  is found. Recent work (6) has shown that two GPDH isozymes exist in WI-38 and SV40 transformed WI-38; thus, the isozyme theory may explain the cause of the intermediate plateau in the G-6-P saturation curve. However, purification and kinetic analysis of GPDH from these cells is necessary in order to prove the isozyme explanation. Comparison of this work to that on human erythrocytes (41) indicates a difference in the  $\text{NADP}^+$  saturation for both sources even though Luzzatto's  $K_s$  at high concentration of  $\text{NADP}^+$  agrees quite well with this work.

From Table 7, it is evident that only inorganic phosphate (1.0 mM) inhibited GPDH. This inhibition was approximately 30% in both cell types at enzyme saturating levels of  $\text{NADP}^+$  and G-6-P. The physiological significance of this inhibition is not clear.

The final enzyme to be discussed is PK. Since PK did not show any statistical variation from both cell sources it was not surprising that the substrate  $K_m$ 's as well as the pH profiles were identical. The pH profile is the sharpest of the four enzymes examined with the pH optimum range 7.0 to 7.5. From Table 4, it is evident that the interaction coefficient for PEP and ADP in both sources is nearly 2.0. The implication is that there are at least two interacting binding sites for ADP and PEP in both types of cells. For

WI-38 and WI-38 VA13A the  $K_m$  for ADP was roughly 0.30 to 0.40 mM which compares closely with the  $K_m$  from rabbit muscle, 0.30 mM, (8) and human red blood cells, 0.33 mM, (30). The  $K_m$  for PEP for the human embryonic lung cells, 0.26 mM, compares favorably with that for rat liver PK, 0.10 to 0.30 mM, (5, 60).

Of the enzymes studied PK proved to be regulated to the greatest extent. PK from both sources was activated by potassium ions ( $K^+$ ), (see Figure 26) and FDP, (see Figure 20). Also, PK from both sources was inhibited by L-alanine and ATP, (see Figures 15-19 and 21-25). For  $K^+$  activation (10 fold) it was found that the enzyme from either source was saturated at a concentration of 50 mM KCl and that the enzyme was one-half saturated at 10 mM KCl. Also, it was found that at enzyme saturating levels of  $NH_4^+$  a 2 fold activation was observed and for  $Na^+$  no effect was observed, respectively. The effect of  $K^+$  ions has been documented for PK from other sources: erythrocyte PK was activated by  $K^+$  and  $NH_4^+$  (30), rat liver PK requires a monovalent cation  $K^+$  or  $NH_4^+$  with  $NH_4^+$  more efficient than  $K^+$  (12), yeast PK is strongly activated by  $K^+$  and  $NH_4^+$  with  $NH_4^+$  having about one-half the activating potential of  $K^+$  (28), and both rabbit muscle and Ehrlich ascites-tumor cells have an absolute requirement for a monovalent ion either  $K^+$  or  $NH_4^+$  is equally effective (11). The  $K^+$  requirement or  $K^+$  activation of PK is possibly related to the

electrolyte pump mechanism of cells. That is, in order to maintain a high intercellular level of  $K^+$  an ATP dependent ion translocation mechanism is used by the cell. Thus, the  $K^+$  activation of PK would result in greater regeneration of ATP and would help maintain the ATP level necessary to maintain a proper intracellular  $K^+$  level. The other activator of PK activity, FDP, in both cells seems to be a common activator of regulated PK's from a variety of sources, e.g. rat liver (5, 38, 59, 61), yeast (25), E. coli (42), mouse liver (38). Weber and co-workers have done extensive work on the regulation of PK from rat liver (59, 61). They found a 1.9 fold stimulation by FDP which appeared as a mixed activator with respect to PEP (59). By comparison, for the human embryonic lung cells the stimulation by FDP was 2 fold and FDP (1.0 mM) appears to be a noncompetitive activator with respect to PEP (see Figure 20). As shown in Figure 27, the FDP activation of PK is greatly reduced by storage. This sensitivity implies that the FDP binding site is a very sensitive allosteric binding site. Weber et al. also found that ATP inhibition was 37% and mixed with respect to enzyme saturating levels of ADP and 61% and noncompetitive with respect to enzyme saturating levels of PEP (59). For PK described in this dissertation ATP was a noncompetitive inhibitor with respect to both substrates and the degree of inhibition was approximately 50% at 1 mM ATP. For rat liver Weber and co-workers found that L-alanine was a

competitive inhibitor (61). However, it was found in this study that L-alanine was non-competitive with respect to both substrates and the degree of inhibition by L-alanine (1 mM) was approximately 50%.

The physiological significance of FDP activation, L-alanine inhibition, and ATP inhibition is more obvious than for  $K^+$  activation. From a glycolytic standpoint the significance of FDP stimulation of PK is evident, i.e. it is a forward feed to improve the efficiency of glycolysis. However, as was pointed out by Weber (59) under conditions of gluconeogenesis this is an undesirable property. He suggested that inhibition of PK by free fatty acids, which are more prevalent under gluconeogenic conditions, offsets FDP activation of PK, and thus, permits FDP to be utilized in gluconeogenesis. Even though ATP and L-alanine were not shown to antagonize FDP activation of human embryonic lung PK, it is probable that the existence of intracellular levels of ATP and L-alanine higher than normally tolerated could result in preferential utilization of FDP in gluconeogenesis. Of course, it is reasonable to assume that when intracellular conditions are suitable for gluconeogenesis the intracellular levels of ATP and L-alanine would be maximal and more likely to be inhibitory levels. From a glycolytic standpoint ATP and L-alanine appear to be classic feedback inhibitors (2). The inhibition of PK by ATP fits in quite well with Atkinson's adenylate control hypothesis



for glycolysis (3) (AMP stimulates the unique glycolytic enzyme of hexose phosphate utilization and ATP inhibits the unique glycolytic enzyme of triose phosphate utilization). The end result being adenylate modulation of the unique enzymes of glycolysis and of ATP production by glycolysis and respiration. The inhibition of PK by L-alanine can also be interpreted as end product control of its own biosynthesis. Thus, the net result of L-alanine and ATP inhibition of PK is inhibition of glycolysis and creation of conditions suitable for gluconeogenesis.

## CHAPTER VI

### SUMMARY

Results, conclusions, and speculations concerning the biochemical differences and similarities with respect to glycolysis and glycolytic regulation were studied using the human diploid cell line WI-38 and its SV40 transformed counterpart WI-38 VA13A. In particular it was found that under the described culturing conditions that WI-38 has approximately a 2.5 fold greater rate of lactate production and glucose utilization. The adenine nucleotide levels were found to be significantly different. Speculations are offered to explain these differences. The specific activities of the glycolytic enzymes with the exception of enolase and phosphoglyceromutase were measured. Also, the levels of GPDH and 6PGADH of the hexose monophosphate shunt were determined. The specific activities of HK, FDPase, GAPDH, GPDH, and 6PGADH measured for both cell types were found to be statistically different. The implications of these results are discussed in connection with glycolysis in both cell types.

Of the enzymes that were shown to have specific activities that were statistically different between both cells, only FDPase was not studied. FDPase was not studied because of its very low activity in the cell free preparation. In order to determine any kinetic similarities or differences pH profiles and saturation curves were made for these enzymes in both cell sources. From the data collected for the saturation curves, Hill plots and Lineweaver-Burk plots were made. In addition to determining kinetic parameters of these enzymes a comprehensive study was undertaken to compare their regulation by small molecular weight metabolites. Speculation is offered on whether the difference in the enzyme profiles is due to an increase in the biosynthesis of the affected enzymes or biosynthesis of an isozyme which has a specific activity that could produce the observed increase or decrease in specific activity. It was concluded that at least under our cultivation conditions a correlation of increased glycolysis to neoplastic transformation cannot be made for the WI-38 and WI-38 VA13A set as can be made for Rous sarcoma or polyoma viral transformed cells.

Examination of PK indicated that it is highly regulated in both types of cells. The physiological significance of this regulation by adenosine triphosphate, L-alanine, and fructose diphosphate was discussed in relation to glycolysis and gluconeogenesis.

The G-6-P saturation curve of GPDH was found to have an intermediate plateau region. The significance and cause of such a region were discussed.

## BIBLIOGRAPHY

1. Aaronson, Stuart A. and Todaro, George J., "Human Diploid Cell Transformation by DNA Extracted from the Tumor Virus SV40," Science, 166, 390 (1969).
2. Atkinson, D. E., "Regulation of Enzyme Activity," Ann. Rev. Biochem., 35, 85 (1966).
3. Atkinson, Daniel E., Hathaway, James A., and Smith, Eddie C., "Kinetics of Regulatory Enzymes," J. Biol. Chem., 240, 2682 (1965).
4. Ashmore, James, Weber, George, Banerjee, Gouri, and Love, William C., "Glucose Metabolism of Tumors Induced by Rous Sarcoma Virus II. Isotope Studies of Alternate Pathways," J. Nat. Cancer Inst. 27, 597 (1961).
5. Bailey, E., Stripe, F., and Taylor, C. B., "Regulation of Rat Liver Pyruvate Kinase," Biochem. J., 108, 427 (1968).
6. Bartholomew, Eleanor M., Bartholomew, William R., and Rose, Noel R., "Isoenzyme Differences Between A Human Diploid Cell Line, WI-38, and SV40 Transformed WI-38," J. Immun., 103, 787 (1969).
7. Bondi, Elliott, W., Watkins, James, Kirtley, Mary E., "Comparison of the Activity of Glyceraldehyde-3-Phosphate Dehydrogenase in Rabbit Tissues," Biochim. Biophys. Acta, 185, 305 (1969).
8. Boyer, P. D., "Pyruvate Kinase," The Enzymes, 6, 107 (1962).
9. Broadfoot, M., Walker, P., Paul, J., Macpherson, I, Stoker, M., "Glycolysis and Respiration of Transformed BHK 21 Cells," Nature, 204, 79 (1964).
10. Burk, Dean and Woods, Mark, "Newer Aspects of Glucose Fermentation in Cancer Growth and Control," Archiv. für Geschwulstforschung, 28, 305 (1967).

11. Bygrave, F. L., "Studies on the Interaction of Metal Ions with Pyruvate Kinase from Ehrlich Ascites - Tumour Cells and from Rabbit Muscle," Biochem. J., 101, 488 (1966).
12. Carminatti, H., De Asua, Luis Jimenez, Recondo, E., Passeron, S., and Rozengurt, E. "Some Kinetic Properties of Liver Pyruvate Kinase (Type L)," J. Biol. Chem., 243, 3051 (1968).
13. Coe, Elmon L., "Correlations Between Adenine Nucleotide Levels and the Velocities of Rate - Determining Steps in the Glycolysis and Respiration of Intact Ehrlich Ascites Carcinoma Cells," Biochim. Biophys. Acta, 118, 495 (1966).
14. Cristofalo, V. J., "Enzymes of Glucose Metabolism in Normal Diploid and Virus - Transformed Human Cells," Proc. 20th Ann. Meeting Tissue Culture Assoc., p. 60 (1969).
15. Cristofalo, V. J., Kabakjian, J. R., and Kritchevsky, D., "Enzyme Activities of Some Cultured Human Cells," Proc. Soc. Exp. Biol. Med., 126, 273 (1967).
16. Cristofalo, V. J. and Kritchevsky, D., "Growth and Glycolysis in the Human Diploid Cell Strain WI-38," Proc. Soc. Exp. Biol. Med., 118, 1109 (1965).
17. Cristofalo, V. J. and Kritchevsky, D., "Respiration and Glycolysis in the Human Diploid Cell Strain WI-38," J. Cell. Physiol., 67, 125 (1966).
18. Cristofalo, V. J., Parris, N., and Kritchevsky, D., "Enzyme Activity during the Growth and Aging of Human Cells in Vitro," J. Cell. Physiol., 69, 263 (1967).
19. Deal, W. C., Jr., "Reversible Dissociation of Tetrameric Rabbit Muscle Glyceraldehyde-3-Phosphate Dehydrogenase into Dimers and Monomers by ATP," J. Biol. Chem., 244, 5695 (1969).
20. Eddy, B., Borman, G., Berkely, W., and Young, R., "Tumors Induced in Hamster by Injection of Rhesus Monkey Kidney Cell Extracts," Proc. Soc. Exp. Biol. Med., 107, 191 (1961).
21. England, P. J., "Effectors of Rat - Heart Hexokinases and Control of Rates of Glucose Phosphorylation in the Perfused Rat Heart," Biochem. J., 105, 907 (1967).

22. Girardi, A. J., Jensen, F. C., and Koprowski, H., "SV40-Induced Transformation of Human Diploid Cells Crises and Recovery," J. Cell. Comp. Physiol., 65, 69 (1965).
23. Girardi, A. J. Sweet, B. H., Slotnick, V. B., and Hilleman, B., "Development of Tumors in Hamsters Inoculated in the Neonatal Period with Vacuolating Virus SV40," Proc. Soc. Exp. Biol. Med., 109, 649 (1962).
24. Habel, Karl, "Specific Antigens Produced by Oncogenic Viruses," in Kirsten, W. H., Malignant Transformation by Viruses, p. 60, Springer-Verlag, New York, Inc., New York (1966).
25. Haeckel, Rainer, Hess, Benno, Lauterborn, Werner, Wuster, Karl-Hans, "Purification and Allosteric Properties of Yeast Pyruvate Kinase," Hoppe-Seyler's Z. Physiol. Chem., 349, 699 (1968).
26. Hayflick, L. and Moorhead, P. S., "The Serial Cultivation of Human Diploid Cell Strains," Exp. Cell Res., 585 (1961).
27. Horecker, B. L. and Kornberg, A., "The Extinction Coefficients of the Reduced Band of Pyridine Nucleotides," J. Biol. Chem., 175, 385 (1948).
28. Hunsley, J. R., and Suelter, C. H., "Yeast Pyruvate Kinase II. Kinetic Properties," J. Biol. Chem., 244, 4819 (1969).
29. Hunter, A. R. and Jefferson, L. S., "Role of Adenosine Monophosphate in Regulation of Metabolic Pathways of Perfused Rat Liver," Biochem. J., 111, 537 (1969).
30. Ibsen, K. H., Schiller, K. W. and Venn-Watson, E. A., "Stabilization, Partial Purification, and Effects of Activating Cations, ADP, and PEP on the Reaction Rates of an Erythrocyte Pyruvate Kinase," Arch. Biochem. Biophys., 128, 583 (1968).
31. Jensen, F., Koprowski, H., and Ponten, J. A., "Rapid Transformation of Human Fibroblast Cultures by Simian Virus 40," Proc. Natl. Acad. Sc., 50, 343 (1963).
32. Joshi, M. B. and Jagannathan, V., "Properties and Kinetics of Purified Brain Hexokinase," Arch. Biochem. Biophys. 125, 460 (1968).

33. Kalckar, Herman M., "Differential Spectrophotometry of Purine Compounds by Means of Specific Enzymes," J. Biol. Chem., 167, 445 (1947).
34. Koprowski, Hilary, Ponten, Jan A., Jensen, Fred, Ravdin, Robert G., Moorhead, Paul, and Saksela, Eero, "Transformation of Cultures of Human Tissue Infected with Simian Virus SV40," J. Cell. and Comp Physiol, 59, 281 (1962).
35. Kornberg, A., "Enzymatic Synthesis of DPN," J. Biol. Chem., 182, 779 (1950).
36. Kruse, Paul F., personal communication.
37. Kruse, Paul F. Jr., and Miedema, Ed, "Glucose Uptake Related to Proliferation of Animal Cells 'in vitro'," Proc. Soc. Exp. Biol. Med., 119, 1110 (1965).
38. Leveille, G. A., "The Influence of FDP on Pyruvate Kinase Activity in Liver, Muscle, and Adipose Tissue of the Rat, Mouse, Pig, and Chicken," Comp. Biochem. Physiol., 28, 773 (1969).
39. Levintow, Leon and Eagle, Harry, "Biochemistry of Cultured Mammalian Cells," in Ann. Rev. Biochem., 30, 605 (1961).
40. Lineweaver, H. and Burk, D., "The Determination of Enzyme Dissociation Constants," J. Amer. Chem. Soc., 56, 658 (1934).
41. Luzzatto, L., "Regulation of the Activity of Glucose-6-phosphate Dehydrogenase by NADP<sup>+</sup> and NADPH," Biochim. Biophys. Acta, 146, 18 (1967).
42. Maeba, P. and Sanwal, B. D., "The Regulation of Pyruvate Kinase of Escherichia coli by Fructose Diphosphate and Adenylic Acid," J. Biol. Chem., 243, 448 (1967).
43. Miedema, E. and Kruse, P. F., "Enzyme Activities and Protein Contents of Animal Cells Cultured Under Perfusion Conditions," Biochem. Biophys. Res. Comm., 20, 528 (1965).
44. Morris, H. P., "Studies on the Development, Biochemistry, and Biology of Experimental Hepatomas," Adv. Cancer Res., 9, 227 (1965).



45. Nagradova, N. K., Vorona, M. K., Asriyants, R. A., "Effect of Adenine Nucleotides on the Activity of Glyceraldehyde-3-Phosphate Dehydrogenases from Different Sources," Biokhimiya, 34, 627 (1969) via Chem. Absts. 71:46116m.
46. Paul, J., Broadfoot, M. M., and Walker, P., "Increased Glycolytic Capacity and Associated Enzyme Changes in BHK21 Cells Transformed with Polyoma Virus," Int. J. Cancer, 1, 207 (1966).
47. Ponten, J., Jensen, F., and Koprowski, H., "Morphological and Virological Investigation of Human Tissue Cultures Transformed with SV40," J. and Cell. Comp. Physiol., 61, 145 (1963).
48. Report of the Commission on Enzyme of the International Union of Biochemistry, New York: Pergamon Press, 1961.
49. Rose, I. A., and O'Connell, E. L., "The Role of Glucose-6-Phosphate in the Regulation of Glucose Metabolism in Human Erythrocytes," J. Biol. Chem., 239, 12 (1964).
50. Shonk, Carl E., and Boxer, George E., "Enzyme Patterns in Human Tissues. I. Methods for Determination of Glycolytic Enzymes," Cancer Research, 27, 709 (1964).
51. Stancel, George M., and Deal, W. C., Jr., "Metabolic Control and Structure of Glycolytic Enzymes. V. Dissociation of Yeast Glyceraldehyde-3-Phosphate Dehydrogenase into Subunits at ATP," Biochem Biophys. Res. Comm., 31, 398 (1968).
52. Steck, Theodore L., Kaufman, Seymour, and Bader, John P., "Glycolysis in Chick Embryo Cell Cultures Transformed by Rous Sarcoma Virus," Cancer Research, 28, 1611 (1968).
53. Teipel, John and Koshland, D. E., Jr., "The Significance of Intermediary Plateau Regions in Enzyme Saturation Curves," Biochemistry, 8, 4656 (1969).
54. Todaro, G. J., Wolman, S. R., and Green, H., "Rapid Transformation of Human Fibroblasts with Low Growth Potential into Established Lines by SV40," J. Cell. Compar. Physiol. 62, 257 (1963).
55. Uyeda, K. and Racker, E., "Regulatory Mechanisms in Carbohydrate Metabolism VII. Hexokinase and Phosphofructokinase," J. Biol. Chem., 240, 4682 (1965).

56. Warburg, O., The Metabolism of Tumors, trans by F. Dickens. London, Constable Press, 1930.
57. Watkins, J. F. and Dulbecco, R., "Production of SV40 Virus in Heterokaryons of Transformed and Susceptible Cells," Proc. Natl. Acad. Sci. U.S., 58, 1396 (1967).
58. Weber, George, Banerjee, Gouri, Levine, Alvin S., and Ashmore, James, "Glucose Metabolism of Tumors Induced by Rous Sarcoma Virus. III. Carbohydrate Metabolic Enzymes in Rous Sarcoma," J. Nat. Cancer Inst., 27, 869 (1961).
59. Weber, George, Lea, Michael A., Convery, Hazel J. Hird, and Stamm, Nancy B., "Regulation of Gluconeogenesis and Glycolysis: Studies of Mechanisms Controlling Enzyme Activity," Advan. Enzyme Regulation, 5, 257 (1967).
60. Weber, George, Lea, Michael A., and Stamm, Nancy B., "Inhibition of Pyruvate Kinase and Glucokinase by Acetyl CoA and Inhibition of Glucokinase by Phosphoenolpyruvate," Life Sci., 6, 2441 (1967).
61. Weber, George, Lea, Michael A., Stamm, Nancy B., "Sequential Feedback Inhibition and Regulation of Liver Carbohydrate Metabolism Through Control of Enzyme Activity," Advan. Enzyme Regulation, 6, 101 (1968).
62. Weber, G., Singhal, R. L., Stamm, N. B., Lea, M. A., and Fisher, E. A., "Synchronous Behavior Pattern of Key Glycolytic Enzymes," Advan. Enzyme Regulation, 4, 59 (1966).
63. Westphal, H. and Dulbecco, R. "Viral DNA in Polyoma and SV-40 Transformed Cell Lines," Proc. Natl. Acad. Sci. U.S., 59, 1158 (1968).
64. Yang, Shih Tzy and Deal, W. C., Jr., "Metabolic Control and Structure of Glycolytic Enzymes. VI. Competitive Inhibition of Yeast Glyceraldehyde-3-Phosphate Dehydrogenase by Cyclic Adenosine Monophosphate, Adenosine Triphosphate, and other Adenine - Containing Compounds," Biochemistry, 8, 2806 (1969).